

MICROCOPY RESOLUTION TEST CHART
NATIONAL BUREAU OF STANDARDS 1963-A

AD-A186 691

OTIC FILE COPY

12

REPORT DOCUMENTATION PAGE

1a. REPORT SECURITY CLASSIFICATION UNCLASSIFIED		1b. RESTRICTIVE MARKINGS	
2a. SECURITY CLASSIFICATION AUTHORITY		3. DISTRIBUTION / AVAILABILITY OF REPORT UNLIMITED	
2b. DECLASSIFICATION / DOWNGRADING SCHEDULE		5. MONITORING ORGANIZATION REPORT NUMBER(S)	
4. PERFORMING ORGANIZATION REPORT NUMBER(S) FINAL		7a. NAME OF MONITORING ORGANIZATION Office of Naval Research	
6a. NAME OF PERFORMING ORGANIZATION C.E. Myers, Chem. Dept., State Univ. of NY, Univ. Ctr. at Binghamton		7b. ADDRESS (City, State, and ZIP Code) 800 North Quincy Street Arlington, VA 22217	
6c. ADDRESS (City, State, and ZIP Code) Binghamton, NY 13901		9. PROCUREMENT INSTRUMENT IDENTIFICATION NUMBER N00014-82-K-0501	
8a. NAME OF FUNDING / SPONSORING ORGANIZATION See 7a		10. SOURCE OF FUNDING NUMBERS	
8b. OFFICE SYMBOL (if applicable)		PROGRAM ELEMENT NO.	PROJECT NO.
8c. ADDRESS (City, State, and ZIP Code) See 7b		TASK NO. NR625-827	WORK UNIT ACCESSION NO.
11. TITLE (Include Security Classification) Cohesive Energies of Transition Metal Silicides and Phosphides (Unclassified)			
12. PERSONAL AUTHOR(S) C.E. Myers, Principal Investigator			
13a. TYPE OF REPORT Technical	13b. TIME COVERED FROM 07/02/82 TO 06/30/87	14. DATE OF REPORT (Year, Month, Day) September 30, 1987	15. PAGE COUNT 49 (incl. figs.)
16. SUPPLEMENTARY NOTATION Supported in part by IBM Corporation and by U.S. Department through Associated Western Universities, Los Alamos National Laboratory and Lawrence Berkeley Laboratory			
17. COSATI CODES			18. SUBJECT TERMS (Continue on reverse if necessary and identify by block number) Transition metal silicides, transition metal phosphides, mass loss knudsen effusion, knudsen effusion mass spectrometry, vaporization behavior, congruent vaporization, thermodynamic activities, phase equilibria, free energy of formation, enthalpy of formation, trends in stability.
FIELD	GROUP	SUB-GROUP	
19. ABSTRACT (Continue on reverse if necessary and identify by block number) Vaporization studies have been carried out by mass loss Knudsen effusion on the Ni-P and Cr-P systems and by Knudsen effusion mass spectrometry on the V-Si, Cr-Si and Ti-Si systems. The experimental data were used to calculate enthalpies of formation of the intermediate phases in these systems. The stabilities of the 1:1 compounds, expressed as enthalpies of atomization, have been compared with each other and with data on silicides, phosphides, and sulfides from the literature to assess factors for inclusion in a phenomenological model for stability. These factors include a) the number and type of bonding electrons, b) effective nuclear charges, c) valence state energies, d) the degree of partial electron transfer with a resulting Madelung energy, and e) contributions from Lewis acid-base interactions involving back-donation of electrons.			
20. DISTRIBUTION / AVAILABILITY OF ABSTRACT <input type="checkbox"/> UNCLASSIFIED / UNLIMITED <input checked="" type="checkbox"/> SAME AS RPT <input type="checkbox"/> DTIC USERS		21. ABSTRACT SECURITY CLASSIFICATION UNCLASSIFIED	
22a. NAME OF RESPONSIBLE INDIVIDUAL		22b. TELEPHONE (Include Area Code)	22c. OFFICE SYMBOL

12

OFFICE OF NAVAL RESEARCH
Contract N00014-82-K-0501
FINAL TECHNICAL REPORT

COHESIVE ENERGIES OF TRANSITION METAL SILICIDES AND PHOSPHIDES

by

Clifford E. Myers
Department of Chemistry
State University of New York at Binghamton
Binghamton, NY 13901

in association with

Robert J. Kematick, Gary A. Murray, Thomas J. Conti, Greg A. Kisacky,
John K. Klingert, Richard E. Cordes, Jeremy Sloan,
Rakesh Sharma, Gail C. DeFoster, George Pigey

and in collaboration with

Edmund K. Storms, Margaret A. Frisch, Leo Brewer

September 30, 1987

Reproduction in whole or in part is permitted for
any purpose of the United States Government

*This document has been approved for public release
and sale; its distribution is unlimited.

DTIC
ELECTE
S OCT 15 1987 D
H

87 10 7 009

PERSONNEL

Clifford E. Myers*, Principal Investigator

Robert J. Kematick*, Postdoctoral Associate

Gary A. Murray, Graduate Student
Thomas J. Conti, Graduate Student
Greg A. Kisacky*, Graduate Student
Richard E. Cordes*, Graduate Student
Jeremy Sloan*, Graduate Student
Rakesh Sharma*, Graduate Student

John K. Klingert*, Undergraduate Student

Gail C. DeFoster*, Technical Assistant
George Pigey, Technical Assistant (IBM-Yorktown)

in collaboration with

Edmund K. Storms, Los Alamos National Laboratory
Margaret A. Frisch, Thomas J. Watson Research Center, IBM Corp.
Leo Brewer, University of California and Lawrence Berkeley Laboratory

*Supported in part by project funds.



Accession For	<input type="checkbox"/>
NTIS Grant	<input checked="" type="checkbox"/>
DTIC TAB	<input type="checkbox"/>
Unannounced	<input type="checkbox"/>
Justification	<input type="checkbox"/>
Distrib: For	
Avail: For	

A-1

TECHNICAL REPORTS AND PUBLICATIONS

1. C. E. Myers, G. A. Kisacky, and J. K. Klingert, "Vaporization Behavior of Chromium Phosphides", J. Electrochem. Soc., **132**, 236 (1985). Technical Report TR-1, September 1, 1984.
2. E. K. Storms and C. E. Myers, "Thermodynamics and Phase Equilibria in the Vanadium-Silicon System", High Temp. Science, **20**, 87 (1985). Technical Report TR-2, September 1, 1984. Also identified as document number LA-UR-84-1040 of Los Alamos National Laboratory.
3. C. E. Myers and T. J. Conti, "Vaporization Behavior, Phase Equilibria, and Thermodynamic Stabilities of Nickel Phosphides", J. Electrochem. Soc., **132**, 454 (1985). Technical Report TR-3, October 4, 1984.
4. C. E. Myers and R. J. Kematich, "Congruent Vaporization in the V-Si System as Studied by High Temperature Knudsen Cell Mass Spectrometry", Proceedings, 33rd Annual Conference on Mass Spectrometry and Allied Topics, San Diego, CA, May 26-31, 1985, Am. Assn. Mass Spectr., East Lansing, MI, 1986, p. 593. Technical Report TR-4, November 26, 1985.
5. C. E. Myers, G. A. Murray, R. J. Kematich, and M. A. Frisch, "Vaporization Thermodynamics of Chromium Silicides", High Temperature Materials Chemistry-III, Z. A. Munir and D. Cubicciotti, eds., Electrochem. Soc. Softbound Proc. Ser., Pennington, NJ (1986), p.47. Technical Report TR-5, November 26, 1985.
6. C. E. Myers and R. J. Kematich, "Vaporization Thermodynamics in the Vanadium-Rich Portion of the Vanadium-Silicon System by High Temperature Knudsen Cell Mass Spectrometry", J. Electrochem. Soc., **134**, 720 (1987). Technical Report TR-6, September 30, 1986.
7. C. E. Myers, R. J. Kematich, and G. A. Murray, "Thermodynamic Activities, Phase Equilibria, and Stabilities in Transition Metal-Silicon Systems by High Temperature Knudsen Cell Mass Spectrometry", Proceedings, International Conference on User Applications of Alloy Phase Diagrams, ASM Materials Week '86, Lake Buena Vista, FL, October 4-9, 1986, L. Kaufman, ed., ASM International, Metals Park, OH, 1987, p. 105.

ABSTRACT

Vaporization studies have been carried out by mass loss Knudsen effusion on the Ni-P and Cr-P systems and by Knudsen effusion mass spectrometry on the V-Si, Cr-Si and Ti-Si systems. The experimental data were used to calculate enthalpies of formation of the intermediate phases in these systems. The stabilities of the 1:1 compounds, expressed as enthalpies of atomization, have been compared with each other and with data on silicides, phosphides, and sulfides from the literature to assess factors for inclusion in a phenomenological model for stability. These factors include a) the number and type of bonding electrons, b) effective nuclear charges, c) valence state energies, d) the degree of partial electron transfer with a resulting Madelung energy, and e) contributions from Lewis acid-base interactions involving back-donation of electrons.

INTRODUCTION

Models serve two related functions in physical science: development of fundamental insight and prediction of properties of interest. The ultimate goal in developing a model is that both of these will be served in the highest degree possible. For small systems, theorists have been able to obtain results which give both deep physical insight and calculated values of observable quantities which are as accurate as the best measured values. Even for these systems, however, the time investment is significant, and the approach is generally not feasible for those who are primarily experimentalists. For more complicated systems such as solid compounds, the problem of constructing models giving both deep insight and accurate results is even more formidable. Most theories of solids have been "tuned" to a particular set of observables of interest by means of adjustable parameters. One of the least satisfactorily treated properties of solids is cohesive energy. There is a need for models which may be used by experimentalists for purposes of interpreting data, predicting properties of interest, and providing a framework for choosing systems and properties for investigation. Such a model should satisfy a number of criteria: a) it should be straightforward in its application, b) it should be predictive to an acceptable level of accuracy, c) its terminology should be appropriate for bond type, d) it should be consistent with the entire range of experimental results (not only those being calculated), and e) the physics invoked should be properly applied.

The original proposal for this project envisioned the development of a phenomenological model for cohesive energies (expressed as enthalpies of atomization) of compounds of the transition metals with p-block elements based on: a) the binding energy per binding electron in the valence state as a function of atomic number, b) a Madelung energy based on partial charges derived from

the principle of electronegativity equivalence, and c) Lewis acid-base interactions between atoms rich in valence electrons and those which are poor. The development of the model was to be accompanied by an experimental program which would examine its critical features. Enthalpies of atomization were to be derived from the results of experiments employing the techniques of a) mass-loss Knudsen effusion (MLKE), b) Knudsen cell-spectrometry (KCMS), and c) high temperature solid-state galvanic cells. The systems chosen for study were: Cr-Si, V-Si, Cr-P, and V-P.

This report describes results of MLKE studies on both the Ni-P system, which were obtained earlier (2) (prepared for publication as a part of the project) and for the Cr-P system, as well as results of studies by KCMS on the V-Si, Cr-Si, and Ti-Si (preliminary) systems. The V-Si and Cr-Si studies included extended vacuum evaporation experiments which were directed to questions of congruent vaporization. Finally, there is a discussion of the current understanding of the factors affecting stabilities of the target compounds.

EXPERIMENTAL PROCEDURES

Preparation and Characterization of Samples

Phosphide samples were prepared by direct combination of weighed amounts of the elements in evacuated and sealed "Vycor" glass ampoules; the procedures and precautions employed have been described elsewhere (1). Silicide samples were synthesized by arc melting weighed mixtures of the elements under an argon atmosphere. Phase analysis was performed by Debye-Scherrer X-ray powder diffraction. Observed powder patterns were compared with patterns calculated by computer from published structural data. Diffraction patterns were taken of both as-prepared samples and residues from various experiments. Selected

silicide samples were analyzed for the metal by oxidation-reduction titrations and for silicon by means of the inductively coupled plasma (ICP) technique. Details are given in published papers (3,4).

Mass-Loss Knudsen Effusion

The vaporization behavior of the transition metal phosphides was studied by MLKE. The apparatus has been described in earlier publications from this laboratory (1,5). It consists of a vacuum system, an induction heater, and a recording vacuum balance. For the experiments on the Cr-P system, the apparatus was fitted with an eddy current concentrator, and the temperatures were measured by means of a tungsten, 25% rhenium-tungsten, 3% rhenium thermocouple; whereas for the Ni-P experiments, no concentrator was used and a chromel-alumel thermocouple was employed to measure temperatures. The thermocouples were calibrated in the manner described previously (1). Channel-orifice effusion cells were machined from graphite rod, and the cells employed in the Cr-P experiments were fitted with a tantalum liner to prevent the phosphide samples from coming into direct contact with the graphite. The effective orifice areas for the Ni-P experiments were obtained by direct measurement and the raw mass-loss data were corrected for non-orifice effusion as described earlier (1). Effective orifice areas for the Cr-P experiments were obtained by calibration based on published vapor pressure data for KCl (6).

Knudsen Cell-Mass Spectrometry

One set of KCMS experiments on the V-Si system was performed at the Los Alamos National Laboratory (LANL) in collaboration with Dr. E. K. Storms. The LANL instrument consists of a 60° sector, single focusing, magnetic deflection mass spectrometer combined with a Knudsen cell. Although this instrument is similar to the design pioneered by Chupka and Inghram (7), it has a number of

unique features which make it particularly well suited for the direct determination of thermodynamic activities at high temperatures. The instrument is described in a recent paper (8) and references contained therein. Experimental procedures paralleled closely those described below for KCMS measurements made at SUNY-Binghamton. The range of compositions studied was from 18 to 70 atomic percent silicon.

The other set of KCMS experiments on the V-Si system and the bulk of such experiments on the Cr-Si system, as well as the experiments on the Ti-Si system, were carried out at SUNY-Binghamton on a 90° sector, single focusing, high resolution mass spectrometer manufactured by Nuclide Corporation. A block diagram of the data acquisition and control system is given in Figure 1. The sample was placed in a tungsten metal cup within a tungsten metal effusion cell which was heated by radiation from a tungsten helix resistance heating element. The entire furnace assembly was surrounded by tungsten and tantalum radiation shields within a water cooled vacuum enclosure. Temperatures were measured with a tungsten-rhenium thermocouple inserted into the base of the effusion cell; the thermocouple was calibrated by means of an optical pyrometer sighted through the orifice into the interior of the effusion cell. The design of the mass spectrometer was such that the molecular beam from the effusion cell, the path of the ionizing electrons, and the ion beam were all mutually perpendicular. Silicon signals were obtained with ionizing electron energies of 12.5 eV in order to minimize the effects of the mass 28 background. The resolution of the instrument was such that, at this electron energy, the silicon peak at mass 28 was effectively separated from the carbon monoxide/nitrogen peak as shown in Figure 2. An ionizing energy of 30.0 eV was used for the metal data. Ion currents as a function of temperature were obtained for both metal (V, mass 51; Cr, mass 52; Ti, mass 48) and silicon,

mass 28. The range of compositions studied was from 10 to 37 atom percent silicon for the V-Si system, 14-88 a/o for the Cr-Si system, and 41-83 a/o for the Ti-Si system. Immediately before or after measuring the metal or silicon ion intensities over a silicide sample, a sample of elemental metal or silicon was placed in the Knudsen cell, and ion intensities were recorded as a function of temperature. Thermodynamic activities were calculated by comparison to the elements as described below. It should be noted that the same Knudsen cell was used in experiments for both the silicides and the elements, but different tungsten cups were used for the respective metal, silicon, or silicide samples.

Some of the experiments on the Cr-Si system were performed in collaboration with Dr. M. A. Frisch at the Thomas J. Watson Research Center of IBM Corporation. The instrument used for these studies was a quadrupole instrument manufactured by Extranuclear Corporation which was fitted with a vacuum furnace and Knudsen cell assembly. The cell orifice was located on the upper cylindrical wall of the cell used in these experiments whereas in all other experiments it was located in the top center of the cell lid. The sample was placed in a tungsten metal cup which was positioned in a tungsten Knudsen cell. The cell was heated by means of a tungsten mesh resistance furnace surrounded by a tungsten and tantalum radiation shield assembly. Again, the entire shield and furnace assembly was contained within a water cooled vacuum enclosure. The temperature was measured with a tungsten-rhenium thermocouple inserted into the base of the Knudsen cell. The calibration of the thermocouple was checked periodically against the melting point of a gold standard. As with the magnetic sector instrument at SUNY-Binghamton, the molecular, electron, and ion beams were mutually perpendicular. Again, to minimize the effect of mass 28 background the silicon signals were obtained with ionizing

electron energies of 12.5 eV. Since the chromium and silicon were measured within the same mass spectral run an ionizing energy of 12.5 eV was also used to obtain the chromium signal.

Extended Heating Experiments

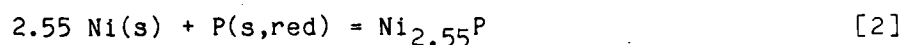
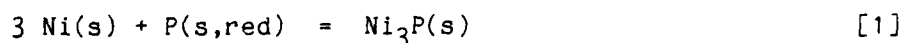
In another group of experiments, samples in open tungsten cups were heated for extended periods either in an induction vacuum furnace (Cr-Si system) or in the mass spectrometer furnace (V-Si system) to examine compositional changes induced by vaporization. For the Cr-Si system the temperature range was 1648-1663K and heating times were 30-40 hours, whereas for the V-Si system heating times ranged from 120 hours at 1900K to 12 hours at 2100K. Compositional changes were determined by chemical analysis and confirmed by X-ray diffraction.

RESULTS

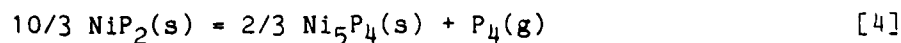
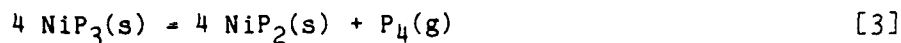
Nickel Phosphides (2,9)

The nickel-phosphorus phase diagram has been well established in the definitive work of Larsson(10), but published data did not permit a complete working out of the thermodynamics of the system. Weibke and Schrag (11) measured directly the heat of reaction of nickel and phosphorus at about 630°C, but their studies were limited to metal-rich compositions. Biltz and Heimbrecht (12) measured dissociation pressures of phosphorus over phosphorus-rich samples, but the static method they employed did not allow an overlap in composition with the calorimetric study (11). The present study was initiated to bridge the gap.

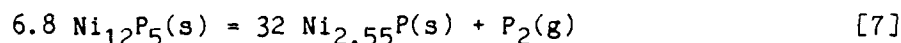
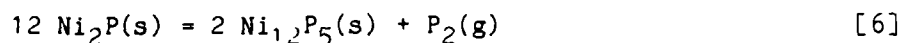
The compositions of the intermediate phases and their temperature ranges of stability were taken from Larsson's study (10); the phase diagram is given in Figure 3. In terms of this diagram, the reactions studied by Weibke and Schrag (11) are:



Similarly, the reactions studied by Biltz and Heimbrecht (12) are:



The effusion study reported here considered the reactions:



which provide a link between the two previous studies.

The primary data were the temperature, corrected for thermocouple calibration, and the rate of mass loss, corrected for non-orifice effusion (1) (less than 20%), obtained from the recording vacuum balance. Detailed results of measurements for reactions [6] and [7] have been published (9). Vaporization was found to be severely retarded and was greatly complicated by sintering of the samples. The former problem was solved by using long channel orifices to achieve equilibrium, and, in dealing with the second, the samples were removed after every second or third pressure determination for regrinding. These necessary measures had the effect of making it very difficult to detect subtle changes in rate of mass loss, and hence of non-equilibrium effects, in the low end of the temperature range.

Pressures of P_2 were calculated, assuming P_2 and P_4 to be in equilibrium in the vapor, by means of the modification of the effusion equation derived earlier (1):

$$\begin{aligned} P(\text{P}_2) &= \frac{K}{2\sqrt{2}} \left\{ \left[1 + \frac{8m}{\alpha K} \left(\frac{\pi RT}{M} \right)^{1/2} \right]^{1/2} - 1 \right\} \\ &= \frac{K}{2\sqrt{2}} \left\{ \left[1 + \frac{Cm}{\alpha K} \left(\frac{T}{M} \right)^{1/2} \right]^{1/2} - 1 \right\} \end{aligned} \quad [8]$$

where K is the equilibrium constant (13) for $\text{P}_4\text{(g)} = 2 \text{ P}_2\text{(g)}$ and M is the

molecular weight of P_2 . When $P(P_2)$ is given in atmospheres, m (the rate of mass loss) in mg/min, T as Kelvin temperature, and a (the effective orifice area) in cm^2 , the constant is $C = 2.127 \times 10^{-6}$. Since the calculated pressures did not show any apparent variation with effective orifice area, all the data were assumed to represent equilibrium conditions. Inasmuch as there were no entropy nor heat capacity data in the literature, these were estimated (1). In addition, the entropy of NiP was adjusted upward by 5% from the original estimate in order to obtain results consistent with the phase diagram. These estimated data have been reported elsewhere (9). Free energies and enthalpies of reaction (298.15K) were calculated by the third-law method for the results described here as well as for the data reported by Biltz and Heimbrecht (12). These data and results of Weibke and Schrag (11), all corrected to 298.15 K, have been published, together with data deduced from the phase diagram (9). The appropriate combinations of the enthalpies of reaction with the enthalpies of formation (13):



yield enthalpies of formation (298.15K):

$$\Delta H_1 = \Delta H_f(Ni_3P) \quad [11]$$

$$\Delta H_2 = \Delta H_f(Ni_{2.55}P) \quad [12]$$

$$\Delta H_{13} = \Delta_f(Ni_{12}P_5) = 1/6.8 ([\Delta H_9 + 32 \Delta H_2 - \Delta H_7]) \quad [13]$$

$$\Delta H_{14} = \Delta H_f(Ni_2P) = 1/12 ([\Delta H_9 + 2 \Delta H_{13} - \Delta H_6]) \quad [14]$$

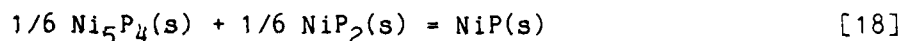
$$\Delta H_{15} = \Delta H_f(Ni_5P_4) = 3/8 [\Delta H_{10} + 20/3 \Delta H_{14} - \Delta H_5] \quad [15]$$

$$\Delta H_{16} = \Delta H_f(NiP_2) = 3/10 [\Delta H_{10} + 2/3 \Delta H_{15} - \Delta H_4] \quad [16]$$

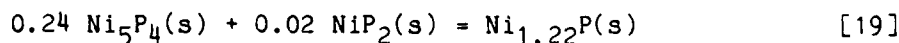
$$\Delta H_{17} = \Delta H_f(NiP_3) = 1/4 [\Delta H_{10} + 4 \Delta H_{16} - \Delta H_3] \quad [17]$$

which are tabulated in Table 1. The enthalpies of formation of NiP and $Ni_{1.22}P$ were deduced from data in Table 1 and the requirements of the phase

diagram (10). Inasmuch as NiP(s) is formed spontaneously from Ni₅P₄ and NiP₂ above (but not below) about 850°C (1123K), its formation from these compounds:



must proceed with positive changes in both enthalpy and entropy at that temperature, and $\Delta H_{18} = T\Delta S_{18}$ at 1123K. This constraint leads to the enthalpy of formation for NiP(s) given in Table 1. Similarly, according to the phase diagram (10), Ni_{1.22}P is stable with respect to Ni₅P₄ and NiP₂ only between about 770°C (1043K) and 825°C (1098K). This requires not only that, for its formation from these compounds:



$\Delta H_{19} = T\Delta S_{19}$ at both these temperatures, but also that both ΔH_{19} and ΔS_{19} be positive at the lower temperature and negative at the higher temperature.

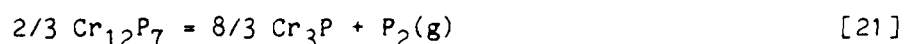
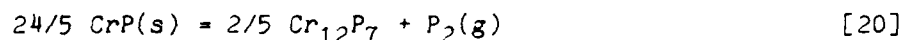
These constraints lead to the enthalpy of formation given in Tables 1.

Chromium Phosphides (14)

Phase relations in the chromium-phosphorus system have been reviewed by Hansen (15), Elliott (16), and Shunk (17). Well-established compounds are Cr₃P, CrP, and CrP₂ which appear to have narrow ranges of homogeneity. Baurecht and coworkers (18) have shown that the compound previously reported as "Cr₂P" is in fact Cr₁₂P₇ with a slight range of homogeneity. The only published stability data were reported by Faller and Biltz (19) who employed a static vapor pressure method to study the dissociation of CrP₂(s) to CrP(s) and P₄(g).

Three univariant composition regions were studied by mass-loss effusion. As established by X-ray powder diffraction, these were CrP-Cr₁₂P₇, Cr₁₂P₇-Cr₃P, and Cr₃P-Cr. The vaporization reactions are inhibited, and equilibrium was demonstrated only for effective orifice areas of $2.39 \times 10^{-4} \text{ cm}^2$ and smaller. The results from the equilibrium runs for the respective two-phase

regions have been published (13). Pressures were calculated by equation [8] from the temperature and rates of mass loss. Inasmuch as there are neither heat capacity nor entropy data for chromium phosphides in the literature, these were estimated (13), and enthalpies of dissociation at 298.15K were calculated by third-law methods. The enthalpy changes (298.15K) for the dissociation reactions:



were used to calculate enthalpies of formation:

$$\Delta H_{23} = \Delta H_f(\text{Cr}_3\text{P}) = 1/2 \Delta H_9 - 1/2 \Delta H_{22} \quad [23]$$

$$\Delta H_{24} = \Delta H_f(\text{Cr}_{12}\text{P}_7) = 3/2 \Delta H_9 + 4 \Delta H_{23} - 3/2 \Delta H_{21} \quad [24]$$

$$\Delta H_{25} = \Delta H_f(\text{CrP}) = 5/24 \Delta H_9 + 1/12 \Delta H_{24} - 5/24 \Delta H_{20} \quad [25]$$

These stability data are tabulated in Table 2. The data for CrP_2 are based on the measurements of Faller and Biltz (19).

Vanadium Silicides (3,8)

Several reviews of the vanadium-silicon system have appeared in the literature (15,16,17,20,21). Although VSi_2 , V_5Si_3 , and V_3Si are well established, there are several matters on which there is less agreement. For example, Hansen (15) shows a wide range of homogeneity for VSi_2 , but Smith (20) reports a negligible range. Conversely, Hansen's phase diagram presents V_3Si as a "line" compound, whereas Smith's shows a range of homogeneity. In addition, Smith's diagram includes V_6Si_5 , but Hansen's does not. Chart (21,22), Freund and Spear (23), and Smith (20) have critically reviewed published thermochemical data for the V-Si system. These data were obtained by combustion calorimetry (24), direct reaction calorimetry (25,26), and EMF measurements (27,28,29). Considerations of both binary (21,22) and ternary

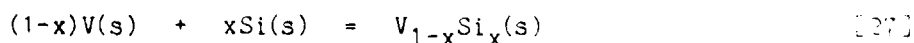
(23) phase diagrams were included in the assessments cited. The EMF data appeared to be most reliable. The heat capacity and entropy data needed to compare results obtained at different temperatures were also reviewed (20-23), and missing data were estimated (20). The present work was directed toward a determination of activities as a function of composition so as to deduce phase boundaries at high temperatures as well as to evaluate free energies and enthalpies of phase formation. Included in the study was the question of the stability of V_6Si_5 .

Thermodynamic activities relative to the pure solid elements were obtained as follows. The partial pressure of a species in a Knudsen cell-mass spectrometry experiment is proportional to IT , where I is the ion current due to that species and T is the temperature of the effusing vapor. Hence the thermodynamic activity of a species in the sample is given by $a = I/I^0$, where I is measured for the element above the sample and I^0 is measured above the pure element under the same experimental conditions of temperature, orifice area, and electron energy (8). Although I and I^0 are measured in different experiments, the mass spectrometer is sufficiently stable that reproducible results are obtained. In practice, activities at a given temperature were calculated from slopes and intercepts of $\log IT$ and $\log I^0T$ vs $1/T$ plots:

$$\log a_i = (A_i - A_i^0)/T + (B_i - B_i^0) \quad [26]$$

where A_i and A_i^0 are the slopes and B_i and B_i^0 are the intercepts of $\log IT$ vs $1/T$ plots for the sample and pure element respectively.

The activities evaluated at 1650K were used to calculate the free energies of formation of the respective vanadium silicides.



$$\Delta G_f^0/R = 2.303 T \log a_V^{(1-x)} a_{Si}^x \quad [28]$$

where x is the atom fraction of Si in the respective solid compound. The geometric mean (average of $\log a$) was used for the activity in the each two-phase region. Entropy and heat capacity data for the silicides cited or estimated by Smith (20) were used, together with Smith's data (30) for V and data from the JANAF Tables (6), to calculate $\Delta H_f^0, 298.15/R$ from the free energy of formation data at 1650K.

Scans with the mass spectrometer established that, at the level of detectability of the instrument, there were no gaseous vanadium-silicon species in the temperature range of the experiments. Typical data are shown in Figure 4. Activities as a function of composition at 1650K are shown in Figure 5. In the work at SUNY-Binghamton the vanadium activity in the V_5Si_3 - V_3Si two-phase region was found to be somewhat greater than was observed at LANL. In addition, at SUNY-Binghamton the variation of the logarithm of the vanadium activity with atom fraction silicon across the V_3Si single-phase region was found to be approximately linear; this permits a much more precise and unambiguous determination of the homogeneity range which was found to extend from 17.5 to 25.5 atom percent silicon at 1800K as shown in Figure 6. Thermodynamic stability data calculated from the experimental results are given in Table 3. Agreement between the LANL and SUNY-Binghamton data is quite good.

The results of the extended heating experiments are shown in Figure 7. The arrows give the direction and extent of composition change during heating; the figures over the arrow are the mass loss and the initial sample mass in milligrams. The temperature uncertainty is ± 10 -20K. Compositions of samples heated at about 1900K and below move past V_5Si_3 toward the V_3Si single-phase region. Above 2000K, compositions move through the V_3Si single-phase region

toward V_5Si_3 .

Chromium silicides (4)

The early work on the chromium-silicon system has been reviewed by Chart (31). The species identified (32) in the chromium-silicon system are Cr_3Si (which exhibits a significant range of homogeneity), Cr_5Si_3 , $CrSi$, and $CrSi_2$ (which also exhibits a homogeneity range). Previous investigations have included combustion calorimetry (33), EMF studies using a fused salt electrolyte (34), effusion vapor pressure experiments on the liquid in the silicon-rich part of the system (35) and effusion studies of the decomposition (36) of $Cr_3Si(s)$. More recently (31), the reaction between the respective silicides and $SiO_2(s)$ giving $SiO(g)$ was also studied by the effusion method. None of these vapor pressure studies used mass spectrometry to confirm the presumed composition of the vapor. Furthermore, the several published results do not show very good agreement. Hence a mass spectrometric investigation of the system was undertaken to attempt resolution of these problems.

Treatment of experimental data paralleled that given above. A plot of log activity as a function of composition at 1500K is given in Figure 8. Free energy functions, $\phi' = -(G^{\circ}_T - H^{\circ}_{298.15})/T$, were evaluated from published thermodynamic data. Details have been published (4). Thermodynamic data for elemental silicon (6) and chromium (37) were taken from the JANAF Tables. The free energy and enthalpy of formation results are given in Table 4. The data published by Chart (30) are included for comparison; agreement is acceptable.

For the samples heated in vacuum for extended periods it was found that samples richer in Cr than $CrSi_2$ lost Cr preferentially, and the samples richer in Si than $CrSi_2$ lost Si preferentially. Hence the samples move toward a congruently vaporizing composition within the $CrSi_2$ single-phase region. The extent of homogeneity of the Cr_3Si and $CrSi_2$ phases is still under

investigation. Figure 9 gives the results of a study of precision lattice constants of rapidly cooled samples whose compositions span the Cr_3Si single phase region. The homogeneity range is approximately 18-26 a/o Si.

Titanium Silicides

The most recent version of the titanium-silicon phase diagram is reported by Svechnikov and coworkers (38). It is based on thermal analysis, microstructures, and X-ray powder diffraction. The compounds in the system are Ti_3Si , Ti_5Si_3 which exhibits a range of homogeneity, Ti_5Si_4 , TiSi , and TiSi_2 . The enthalpy of atomization of TiSi , based on data in the literature (39,40), is higher than would be expected on the basis of the number of bonding electrons, and thus it deserves attention since a significant degree of charge transfer, Ti to Si, would not be expected. The accepted value for the enthalpy of formation of TiSi (41) is based on the study of high temperature solid-state reactions by Brewer and Krikorian (39) and the direct reaction calorimetry of Robins and Jenkins (40). The only study of the thermodynamic stabilities of titanium silicides which has appeared more recently is one which involved measuring the thermodynamics of the simultaneous reduction of titanium and silicon tetrachlorides with sodium metal at 650° (42). The resulting enthalpies of formation appear to be significantly greater than those reported earlier. Since a reliable value of the enthalpy of formation of TiSi is needed in the assessment of trends (particularly as TiSi appears to be pivotal), as well as for practical applications, we have initiated a study of this system.

Difficulties were experienced in demonstrating the presence of Ti_5Si_4 in some of the samples in which it was expected to be present. Although X-ray diffraction peaks were observed for an apparent intermediate phase between Ti_5Si_3 and TiSi , the diffraction pattern did not correspond to that calculated

from published crystallographic data (43). Activities as a function of composition are shown in Figure 10. Even though the now familiar "stair-step" plot is obtained and there is support for a phase between Ti_5Si_3 and $TiSi$, there are some obvious problems. The scatter in the data is significantly greater than was observed for the Cr-Si and V-Si systems. These measurements on titanium silicides were being made during the same time period, on the same instrument, and by means of the same techniques as for measurements on the Cr-Si system. Hence the problems appear to be in the chemistry rather than in the measurements. The tentative experimental data were used to calculate thermodynamic stabilities in the manner described above. There are no absolute entropy data for the titanium silicides in the literature, and these were estimated in comparison with other transition metal silicide systems for which entropies are known. Heat capacity functions were estimated as being additive of the elements. The resulting free energies and enthalpies of formation are given in Table 5. These preliminary results are in reasonable agreement with published data from direct reaction calorimetry. However, additional work must be done on this system to remove ambiguities.

DISCUSSION

Congruent Vaporization

Vaporization behavior in the vanadium-rich portion of the V-Si system may be understood in terms of the schematic pressure vs composition diagrams shown in Figure 11. The use of P-X diagrams to interpret vaporization behavior has been discussed by Gilles (44) among others. We conclude that at 1900K and below congruently vaporizing compositions (the specific composition will depend on temperature) will be found within the V_3Si single-phase region as shown in Figure 11a. This conclusion is based on the considerations: 1) the composition of a sample richer in silicon than V_5Si_3 moves past that composi-

tion toward V_3Si upon extended vaporization, and b) partial pressure ratios (P_{Si}/P_V), calculated from the thermodynamic activity for compositions more vanadium-rich than the V_3Si single-phase region, are orders of magnitude too low for congruent vaporization to occur in this composition range. We term this *congruent vaporization convergent* since the composition will move toward the congruently vaporizing composition upon vaporizing samples of either higher or lower silicon content. For temperatures at or above 2000K we conclude that V_5Si_3 will be congruently vaporizing (and convergent) as shown in Figure 11c. This conclusion is based on the considerations: a) samples richer in vanadium than the V_3Si single-phase region move through that region toward V_5Si_3 upon extended vaporization, and b) calculated partial pressure ratios (P_{Si}/P_V) for samples more silicon-rich than V_5Si_3 are orders of magnitude too high for congruent vaporization to occur. The upper temperature limit of these calculations is the incongruent melting temperature of V_6Si_5 at about 1950K (20). This limit also precluded extended vaporization studies above 1950K on samples more rich in silicon than V_5Si_3 since molten samples attack the tungsten containers. As temperature is raised from 1900K to 2000K there must be a continuous transition from the situation described by Figure 11a to that described by Figure 11c. As a consequence, there must be an intermediate range of temperatures for which Figure 11b applies. In this range both V_3Si and V_5Si_3 contain convergent congruently vaporizing compositions, and there will be a series (with compositions depending on temperature) of local maxima in the total vapor pressure which are congruently vaporizing in the divergent sense. We propose the term euatmotic (Gk. easy vaporizing) for such a local maximum, in parallel with the more familiar term eutectic (Gk. easy melting).

The vaporization characteristics of the V-Si system (at 2000K) are summarized in Figure 12. The two curves in this figure both plot the (P_{Si}/P_V)

ratio in the gas phase vs the X_{Si}/X_V ratio in the condensed phase. Curve I (the "stair-step" curve) may be described by the relation

$$X_{Si}^G/X_V^G = P_{Si}/P_V = (a_{Si}P_{Si}^0)/(a_V P_V^0) \quad [29]$$

where experimentally measured a_{Si} and a_V data and literature P_{Si}^0 and P_V^0 data have been used to calculate the values plotted in the various regions. Curve II is described by

$$X_{Si}^G/X_V^G = P_{Si}/P_V = (X_{Si}^S/X_V^S)(M_{Si}/M_V)^{1/2} \quad [30]$$

which is the relation that must be obeyed if a sample of composition X_{Si}^S is to vaporize congruently under Knudsen conditions. Compositions at which the two plots cross are congruently vaporizing. If Si/V for the vapor is constant (two solid phases) the intersection is the eutmotic composition, whereas if Si/V for the vapor is not constant (one solid phase) the intersection represents a convergent congruently vaporizing composition. While the existence of a single convergent congruently vaporizing composition is common, systems with two such compositions are relatively rare; known examples include some of the rare earth metal-sulfur systems (45,46).

The existence of a congruently vaporizing composition within a metal-silicon system depends upon a rough matching of the volatilities, and hence of sublimation enthalpies, of the metal and silicon. In systems for which the metal has a very low sublimation pressure (such as Ta-Si (47)) silicon will be lost preferentially at all compositions. On the other hand, if the metal is much more volatile than silicon (as in the Mn-Si system (48)), it will be lost preferentially at all compositions. The location of the congruently vaporizing composition within the particular metal-silicon system also depends upon relative volatilities. Since vanadium is less volatile than silicon, the congruently vaporizing compositions in the V-Si system appear in the vanadium-

rich portion. However, in the Cr-Si system, the congruently vaporizing composition is in the CrSi_2 single phase region since chromium is more volatile than silicon.

Stability Factors

As noted above, the present work has sought to identify factors which are candidates for inclusion in a phenomenological model for cohesive energy of binary compounds of the transition metals with p-block elements. Some of those factors have been examined in relation to quantitative correlation of the cohesive energies of the transition metals themselves, while a more qualitative assessment was made for transition metal silicides, phosphides, and sulfides. The factors examined are a) the number and type of bonding electrons, b) effective nuclear charges, c) valence state energies, d) the degree of partial electron transfer with a resulting Madelung energy, and e) contributions from Lewis acid-base interactions involving back-donation of electrons.

The measure of stability chosen was enthalpy of atomization. However, in the atomization process the enthalpy difference being considered is that between the atoms in the compound and ground state atoms. Thus the enthalpy of atomization includes not only the bond enthalpy but also an energy term for relaxation to ground state atoms. Hence this measure of stability may not exhibit trends which can be interpreted in a straightforward manner. See Figure 13 which also includes the enthalpies of sublimation of the respective metals. In all three MX series (X = Si, P, S) the atomization enthalpies parallel the enthalpies of sublimation from Cr to Ni, with the exception of MnS. However, in the early part of the series, ScP, ScS, TiSi, and TiS are all higher than expected on the basis of parallel behavior. The value given for "VSi" is a calculated one based on data for V_6Si_5 since VSi has not been

reported.

The parallel behavior observed, to a degree, between enthalpies of atomization of 1:1 compounds and enthalpies of sublimation of the metals suggests a common basis. For the latter an explanation was proposed by Griffith (49) who showed that the enthalpy of sublimation may be viewed as the difference between a binding enthalpy and a valence state energy (VSE). The former is a function of atomic number, and the latter is the sum of a promotion energy, P , to the lowest term of the valence state configuration, which is presumed in all cases to be $d^{n-1}s$, and the energy, E , necessary to uncouple the spins. Griffith obtained P from spectroscopic tables and calculated E from the appropriate Racah parameters. If the VSEs are added to the respective ΔH_s values, enthalpies of sublimation to hypothetical valence state atoms, ΔH_s^* , are obtained, and these are plotted as designated in Figure 14. There is in this plot a single maximum at Cr which has the greatest number of bonding (unpaired) electrons in the hypothetical valence state. Hence the element with the greatest number of bonding electrons exhibits the greatest cohesive enthalpy. An attempt to make a quantitative correlation proceeded as follows. ΔH_s^* was assumed to be a function of the number of bonding electrons per atom. Inasmuch as electrons of different angular momenta are screened differently by the core electrons, the 4s and 3d electrons were treated separately. A treatment employing one parameter each for 3d and 4s electrons (multiplied by the effective nuclear charge) gives maximum differences between experimental and calculated values in excess of 20 kK. However, inclusion of a constant term for the 3d electrons leads to a maximum difference of less than 8kK and an average difference of 3.2 kK. The results, as shown in Figure 14, are satisfactory in illustrating the validity of the approach.

Enthalpies of atomization of 1:1 compounds to valence state metal atoms

are also shown in Figure 14. In Figure 15 these enthalpies of atomization are plotted as a function of the number of valence electrons (metal plus p-block element). These results lend themselves to qualitative interpretation. For the silicides (CrSi to NiSi), phosphides (CrP to NiP), and sulfides (CrS to NiS, except for MnS) the plots show a regular relationship between the number of bonding electrons and the atomization enthalpy to (metal) valence state atoms. Explanations are needed for enhancement of bond strength in the cases of ScP, ScS, TiSi, TiS, and MnS.

An experimental basis for explaining at least some of the enhanced bond strength may be found in the X-ray photoelectron spectra studied by Franzen and coworkers (50). Shifts in core-level binding energies are interpreted as being due to partial electron transfer. The high value of atomization enthalpy for MnS may be attributed to partial ionic character as evidenced by shifts in the $2p_{3/2}$ X-ray photoelectron spectrum. There is similar evidence that TiSi and particularly ScP have some ionic character. None of these shifts are as great as for Sc_2S_3 , and hence the degree of ionicity for these compounds is not great. The core-level X-ray photoelectron spectra of ScS and TiS, in contrast to MnS, ScP, and TiSi, indicate a small net metal-to-sulfur electron transfer. This is a puzzling result in view of the enhanced bond strength in these compounds. Both Sc and Ti have rather extensive unoccupied d-orbitals and S has lone pairs, the unexpectedly high enthalpies for these compounds may be due to Lewis acid-base interactions involving these orbitals. Indeed a considerable portion of the enhancement of bond strength in ScP may also be due to such interactions. This interpretation is in accord with the results of band structure calculations and measurements of the photoelectron spectra on $ScS_{1.01}$ carried out by Franzen and coworkers (51) who concluded that the bonding in this compound is described in terms of a covalent bonding

component: nonmetal-metal sigma-type bonding (S 2p - Sc 3d e_g) within the valence band states and primarily metal-metal sigma bonding (Sc 3d t_{2g} states) with some nonmetal-metal pi-bonding (S 2p - Sc 3d t_{2g}) within the conduction band states.

ACKNOWLEDGEMENTS

The mass spectrometer employed in the KCMS studies at SUNY-Binghamton was generously donated by Xerox Corporation to the Foundation of the State University of New York at Binghamton. The bulk of the work on the vanadium-silicon system carried out at the Los Alamos National Laboratory was supported by the U. S. Department of Energy through both Associated Western Universities and LANL. Major support for the studies on the chromium-silicon system both at IBM-Yorktown and at SUNY-Binghamton was provided by IBM Corporation in the form of salaried study leave plus material support for Gary A. Murray. The on-going concern to understand trends in stabilities has its roots in work done at SUNY-Binghamton with partial support of the U. S. Department of Energy. The current state of understanding was developed with partial support of the U. S. Department of Energy through Associated Western Universities at both LANL and Lawrence Berkeley Laboratory. The support of the Office of Naval Research provided the principal means for carrying out the research described in this report as well as the flexibility to allow the collaborations which have enhanced its quality and significance. That support is very much appreciated. Finally, the Principal Investigator is pleased to acknowledge those co-workers the results of whose efforts are described here; it has been a happy and productive association.

REFERENCES

1. C. E. Myers, High Temp. Science, **6**, 309 (1974).
2. T. J. Conti, M.A. Thesis, SUNY-Binghamton, 1975.
3. C. E. Myers and R. J. Kematick, J. Electrochem. Soc., **134**, 720 (1987).
Technical Report TR-6, September 30, 1986.
4. C. E. Myers, G. A. Murray, R. J. Kematick, and M. A. Frisch, "High Temperature Materials Chemistry-III", Z. A. Munir and D. Cubicciotti, eds., Electrochem. Soc. Softbound Proc. Ser., Pennington, NJ (1986), p.47.
Technical Report TR-5, November 26, 1985.
5. M. H. Hannay and C. E. Myers, J. Less-Common Met., **66**, 145 (1979).
6. D. R. Stull and H. Prophet, NSRDS-NBS No. **37** (1971).
7. W. A. Chupka and M. G. Inghram, J. Phys. Chem., **59**, 100 (1955).
8. E. K. Storms and C. E. Myers, High Temp. Science, **20**, 87 (1985). Technical Report TR-2, September 1, 1984. Also identified as document number LA-UR-84-1040 of Los Alamos National Laboratory.
9. C. E. Myers and T. J. Conti, J. Electrochem. Soc., **132**, 454 (1985).
Technical Report TR-3, October 4, 1984.
10. E. Larsson, Arkiv Kemi, **23**, 335 (1965).
11. F. Weibke and G. Schrag, Z. Electrochem., **47**, 222 (1941).
12. W. Biltz and M. Heimbrecht, Z. Anorg. Allg. Chem., **237**, 132 (1938).
13. C. E. Myers, G. A. Kisacky, and J. K. Klingert, J. Electrochem. Soc., **132**, 236 (1985). Technical Report TR-1, September 1, 1984.
14. M. Hansen and K. Anderko, "Constitution of Binary Alloys", McGraw-Hill, New York, 1958.
15. R. P. Elliott, "Constitution of Binary Alloys, First Supplement", McGraw-Hill, New York, 1965.
16. F. A. Shunk, "Constitution of Binary Alloys, Second Supplement", McGraw-Hill, New York, 1969.
17. H. E. Baurecht, H. Boller, and H. Nowotny, Monatsh. Chem., **102**, 373 (1971).
18. D. T. Hawkins, "Metals Handbook", Vol. 8, T. Lyman, ed., ASM Intl., Metals Park, OH, 1973, pp. 334, 375.
19. F. E. Faller and W. Biltz, Z. Anorg. Allgem. Chem., **248**, 209 (1941).
20. J. F. Smith, Bull. Alloy Phase Diagrams, **2**, 42 (1981).

21. T. G. Chart, Natl. Phys. Lab. (UK), Rept. 18 (1972).
22. T. G. Chart, High Temp. High Press., **5**, 241 (1973).
23. P. F. Freund and K. E. Spear, J. Less-Common Met., **60**, 185 (1978).
24. Yu. M. Golutvin and T. M. Kozlovskaya, Russ. J. Phys. Chem. (Engl. Transl.), **34**, 1116 (1960).
25. O. Gorelkin and S. Mikhailikov, Russ. J. Phys. Chem., **45**, 1523 (1971).
26. O. Gorelkin, A. Dubrovin, O. Kolensnikova, and N. Chirkov, Russ. J. Phys. Chem., **46**, 431 (1972).
27. V. Eremenko, Dopov. Akad. Nauk Ukr. RSR Ser. B, **36**, 712 (1974).
28. V. Eremenko, G. Lukashenko, and V. Sidorko, Rev. Int. Hautes Temp. Refract., **12**, 237 (1975).
29. V. Eremenko, G. Lukashenko, V. Sidorko, and O. Kulik, Dopov. Akad. Nauk Ukr. RSR Ser. A, **38**, 365 (1976).
30. J. F. Smith, Bull. Alloy Phase Diagrams, **2**, 40 (1981).
31. T. G. Chart, Met. Sci., **9**, 504 (1975).
32. H. J. Goldschmidt and J. A. Brand, J. Less-Common Metals, **3**, 34 (1961).
33. Yu. M. Golutvin and L. Chin-k'uei, Russ. J. Phys. Chem., **35**, 62 (1961).
34. V. N. Eremenko, G. M. Lukashenko, V. R. Sidorko, and A. M. Khar'kova, Sov. Powder Metall. Met. Ceram., **1971**, 563.
35. J.-P. Riegert, A. Vermande, and I. Ansara, High Temp.-High Pressures, **5**, 231 (1973).
36. A. S. Bolgar, S. P. Gordienko, A. A. Lysenko, and V. V. Fesenko, Russ. J. Phys. Chem., **45**, 1154 (1971).
37. M. W. Chase, J. L. Curnutt, H. Prophet, R. A. McDonald, and A. N. Syverud, J. Phys. Chem. Ref. Data, **4**, 1 (1975).
38. V. N. Svechnikov, Yu. A. Kocherzhinskii, L. M. Yupko, O. G. Kulik, and E. A. Shiskin, Dokl. Akad. Nauk SSSR, **193**, 393 (1969).
39. L. Brewer and O. H. Krikorian, J. Electrochem. Soc., **103**, 701 (1956).
40. D. A. Robins and I. Jenkins, Acta Met., **3**, 598 (1955).
41. R. Hultgren, P. D. Desai, D. T. Hawkins, M. Gleiser, and K. K. Kelley, "Selected Values of the Thermodynamic Properties of Binary Alloys," American Society for Metals, Metals Park, OH, 1973.

42. V. D. Savin, Russ. J. Phys. Chem. (Engl. Trans.), **47**, 1423 (1973).
43. J. Nickl and H. Sprenger, Z. Metallk., **60**, 136 (1969).
44. P. W. Gilles, Chap. 2 of "The Characterization of High Temperature Vapors", J. L. Margrave, Ed., Wiley, 1967.
45. E. D. Eastman, L. Brewer, L. A. Bromley, P. W. Gilles, and N. L. Lofgren, J. Am. Chem. Soc., **72**, 2248 (1950).
46. E. D. Cater, B. H. Mueller, and J. A. Fries, "Proceedings, 10th Materials Research Symposium: Characterization of High Temperature Vapors and Gases", J. W. Hastie, Ed., Natl. Bur. Stand. Spec. Publ. **561**, 1979, pp. 237-263.
47. C. E. Myers and A. W. Searcy, J. Am. Chem. Soc., **79**, 526 (1957).
48. H. Nowotny, J. Tomsika, L. Erdelyi, and A. Neckel, Monat. Chem., **108**, 7 (1977).
49. J. S. Griffith, J. Inorg. Nucl. Chem., **3**, 15 (1956).
50. H. F. Franzen and C. Sterner, J. Solid State Chem., **25**, 227 (1978); R. J. Kematick, J. W. Anderegg, H. F. Franzen, and C. E. Myers, unpublished work; C. E. Myers, H. F. Franzen, and J. W. Anderegg, Inorg. Chem., **24**, 1822 (1985).
51. J. Nakahara, D. K. Misemer, and H. F. Franzen, J. Solid State Chem., **61**, 338 (1986).

TABLE 1

THERMODYNAMIC STABILITIES OF NICKEL PHOSPHIDES
Enthalpies of Formation (from red P) at 298.15K

	$-\Delta H_f^\circ/R$
$1/4 \text{ Ni}_3\text{P(s)}$	5.94 ± 0.5
$1/3.55 \text{ Ni}_{2.55}\text{P(s)}$	6.65 ± 0.5
$1/17 \text{ Ni}_{12}\text{P}_5\text{(s)}$	7.73 ± 0.5
$1/3 \text{ Ni}_2\text{P(s)}$	6.87 ± 0.5
$1/9 \text{ Ni}_5\text{P}_4\text{(s)}$	6.39 ± 0.5
$1/2.22 \text{ Ni}_{1.22}\text{P(s)}$	6.32 ± 0.5
$1/2 \text{ NiP(s)}$	6.09 ± 0.5
$1/3 \text{ NiP}_2\text{(s)}$	5.38 ± 0.5
$1/4 \text{ NiP}_3\text{(s)}$	4.52 ± 0.5

Note: Energy data are given in rational units; values in other units may be obtained by multiplying by the appropriate value of the gas constant R.

TABLE 2

THERMODYNAMIC STABILITIES OF CHROMIUM PHOSPHIDES
Enthalpies of Formation (from red P) at 298.15K

	$-\Delta H_f^\circ/R$
$1/2 \text{ CrP(s)}$	5.69 ± 0.18
$1/19 \text{ Cr}_{12}\text{P}_7\text{(s)}$	4.48 ± 0.32
$1/4 \text{ Cr}_3\text{P(s)}$	3.18 ± 0.04
$1/3 \text{ CrP}_2\text{(s)}$	4.8 ± 0.7 *

* Based on data of Faller and Biltz (19).

TABLE 3

THERMODYNAMIC STABILITIES OF VANADIUM SILICIDES

	$-\Delta G_f^\circ, 1650\text{K/R}$ (kK)	Source
1/4 V_3Si	3.63	Si and V activities (22 a/o Si), SUNY
	4.39	Si and V activities (24 a/o Si), SUNY
	4.35	Si and V activities, $V_5Si_3 + V_3Si$ (32 a/o Si), SUNY
	4.40	Si (calc.) and V activities, $V_5Si_3 + V_3Si$, LANL
1/8 V_5Si_3	5.49	Si and V activities, $V_5Si_3 + V_3Si$ (32 a/o Si), SUNY
	5.47	Si (calc.) and V activities, $V_3Si + V_6Si_5$, LANL
1/11 V_6Si_5	5.25	Si and V activities, $V_6Si_5 + VSi_2$, LANL
1/3 VSi_2	4.25	Si and V activities, $V_6Si_5 + VSi_2$, LANL
	$-\Delta H_f^\circ, 298.15/R$ (kK)	
1/4 V_3Si	5.37±0.2	Mean value, this work, SUNY
	5.40±0.2	This work, LANL
	5.18	Smith (20)
1/8 V_5Si_3	6.33±0.2	This work, SUNY
	6.31±0.2	This work, LANL
	6.47	Smith (20)
1/11 V_6Si_5	5.93±0.2	This work, LANL
	5.97	Smith (20)
1/3 VSi_2	4.90±0.2	This work, LANL
	4.90	Smith (20)

TABLE 4

THERMODYNAMIC STABILITIES OF CHROMIUM SILICIDES

	$-\Delta G_f^0, 1500K/R$ (kK)	Source
1/4 Cr ₃ Si	3.39	Si and Cr activities, Cr ₃ Si + Cr ₅ Si ₃
1/8 Cr ₅ Si ₃	3.82	Si and Cr activities, Cr ₃ Si + Cr ₅ Si ₃
	3.82	Si and Cr activities, Cr ₅ Si ₃ + CrSi
1/2 CrSi ₂	3.55	Si and Cr activities, Cr ₅ Si ₃ + CrSi
	3.68	Si and Cr activities, CrSi + CrSi ₂
1/3 CrSi ₂	3.07	Si and Cr activities, CrSi + CrSi ₂
	$-\Delta H_f^0, 298.15/R$ (kK)	
1/4 Cr ₃ Si	3.50±0.2	This work
	3.18	Chart (31)
1/8 Cr ₅ Si ₃	3.46±0.2	Mean value this work
	3.36	Chart (31)
1/2 CrSi	3.20±0.2	Mean value, this work
	3.30	Chart (31)
1/3 CrSi ₂	3.36±0.2	This work
	3.21	Chart (31)

TABLE 5
 THERMODYNAMIC STABILITIES OF TITANIUM SILICIDES
 (Provisional)

	$-\Delta G_f^{\circ}, 1550\text{K/R}$ (kK)	Source
1/8 Ti ₅ Si ₃	7.54	Si and Ti activities, Ti ₅ Si ₃ + Ti ₅ Si ₄
1/9 Ti ₅ Si ₄	7.48	Si and Ti activities, Ti ₅ Si ₃ + Ti ₅ Si ₄
1/2 TiSi	7.09	Si and Ti (calc.) activities, Ti ₅ Si ₄ + TiSi
1/3 TiSi ₂	5.53	Si and Ti (calc.) activities, TiSi + TiSi ₂
	$-\Delta H_f^{\circ}, 298.15/R$ (kK)	
1/8 Ti ₅ Si ₃	7.42	This work
	8.71	Hultgren (41)
1/9 Ti ₅ Si ₄	7.31	This work
1/2 TiSi	7.37	This work
	7.80	Hultgren (41)
1/3 TiSi ₂	5.68	This work
	5.39	Hultgren (41)

FIGURE CAPTIONS

1. Data acquisition and control system.
2. Instrument resolution and electron energy at mass 28.
3. Nickel-phosphorus phase diagram (after Larsson (10)).
Phases: a, Ni_3P ; b, Ni_5P_2 (β); c, $\text{Ni}_{-2.55}\text{P}$; d, Ni_{12}P_5 ; e, Ni_2P ; f, Ni_5P_4 ; g, $\text{Ni}_{-1.22}\text{P}$; h, NiP ; i, NiP_2 ; j, NiP_3 .
4. Typical data: Log IT vs $1/T$ for sample and solid element standards.
5. Log activity vs composition for vanadium-silicon system at 1650K: O = V, X = Si. Large symbols, SUNY-Binghamton (3); small symbols, LANL (8).
6. Log vanadium activity vs composition near V_3Si at 1800K: Squares, SUNY-Binghamton (3); circles, LANL (8).
7. Extended heating experiments: Arrows indicate direction and extent of composition change; in figures over each arrow, numerator is mass loss (mg) and denominator is initial mass of sample.
8. Log activity vs composition for chromium-silicon system at 1500K. Squares, SUNY-Binghamton: open, Cr; filled, Si. Hexagons, IBM: filled, Cr.
9. Homogeneity range of Cr_3Si
10. Log activity vs composition for titanium-silicon system at 1550K.
11. Pressure vs composition (schematic).
12. Gas phase composition ratio, $X_{\text{Si}}/X_{\text{V}}$, at 2000K: I. Observed; II. Calculated for congruent vaporization under effusion conditions.
13. Enthalpies of atomization to ground state atoms.
14. Enthalpies of atomization to valence state metal atoms.
15. Enthalpies of atomization to valence state atoms as a function of valence electron count.

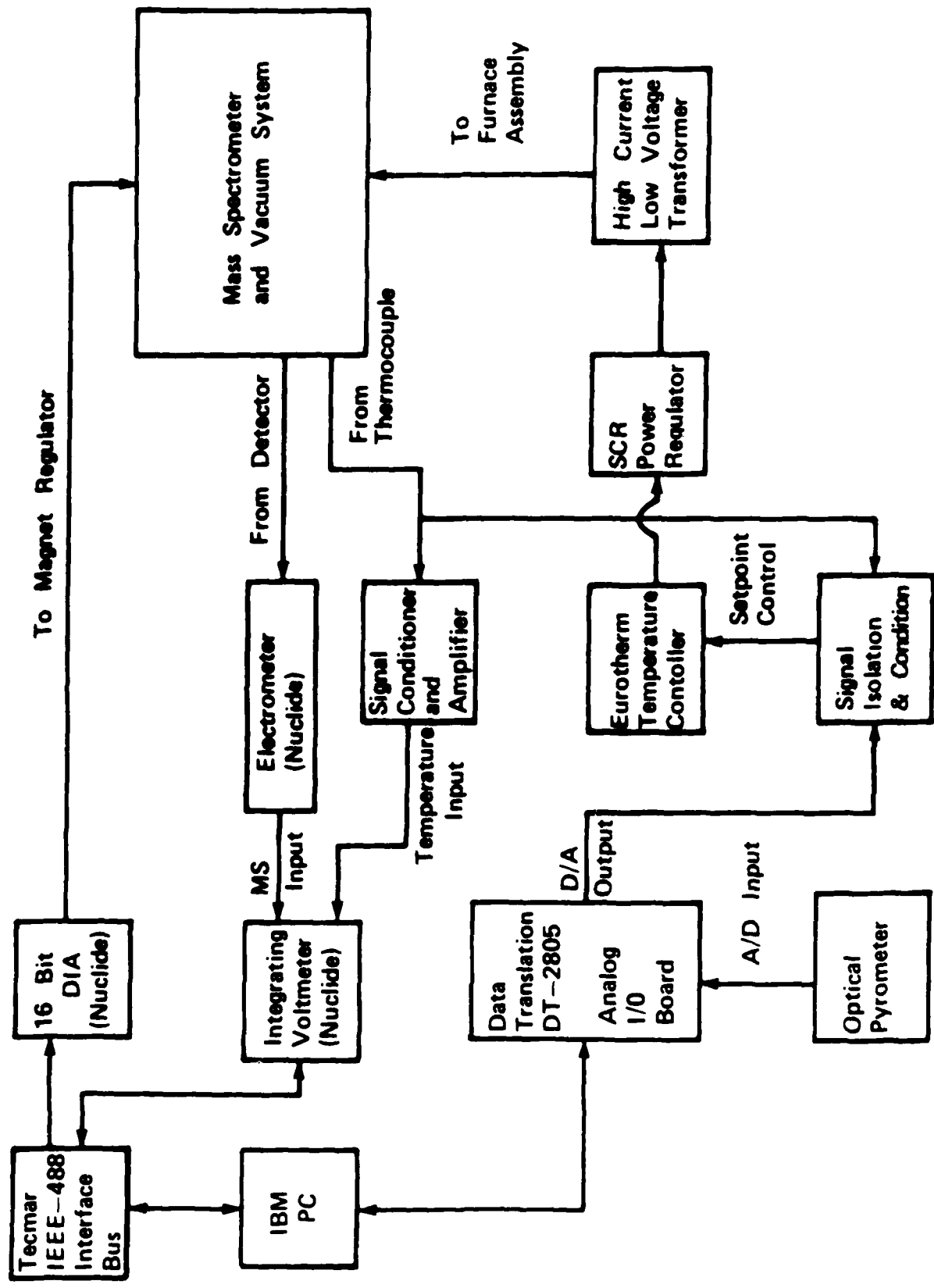


FIGURE 1

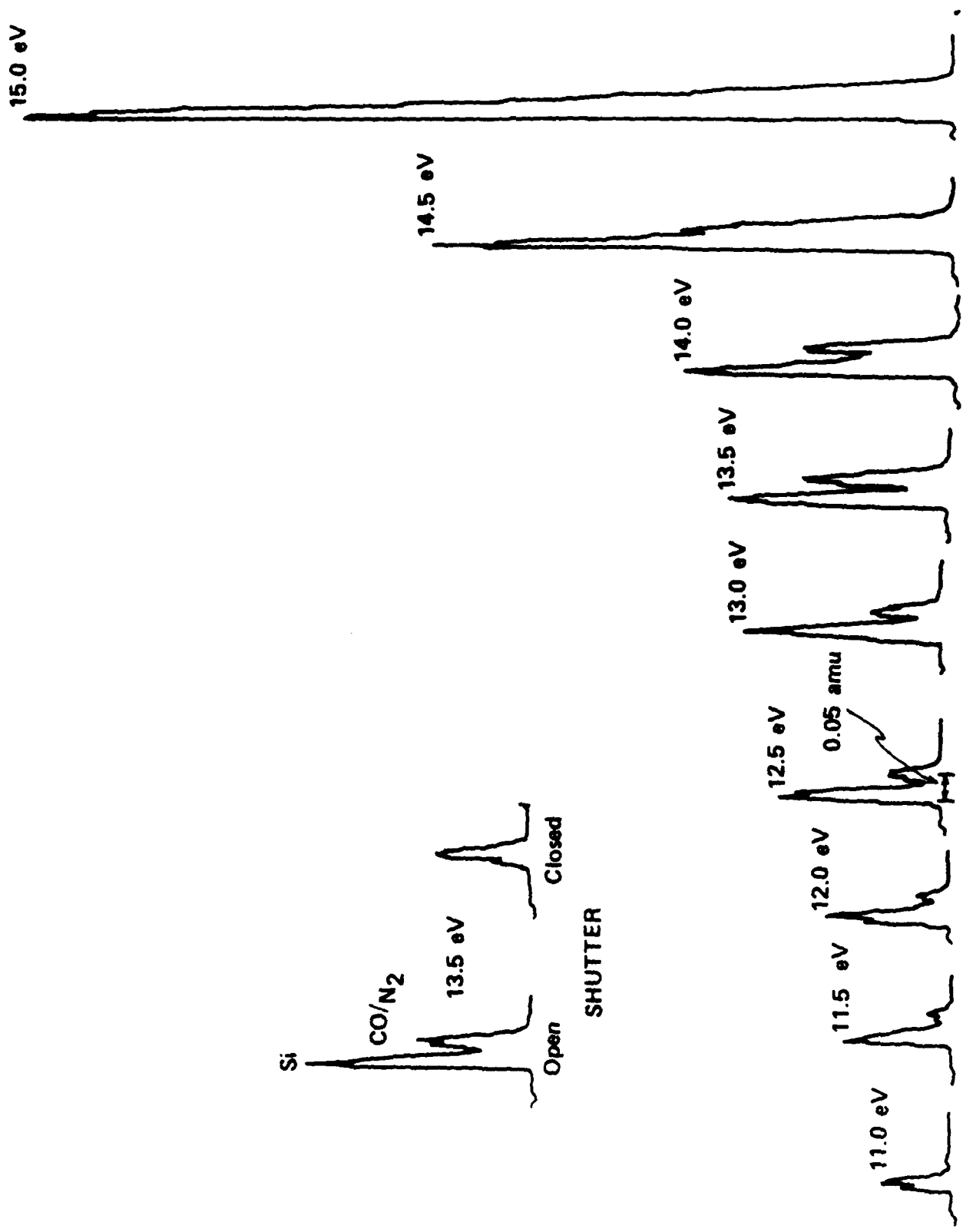


FIGURE 2

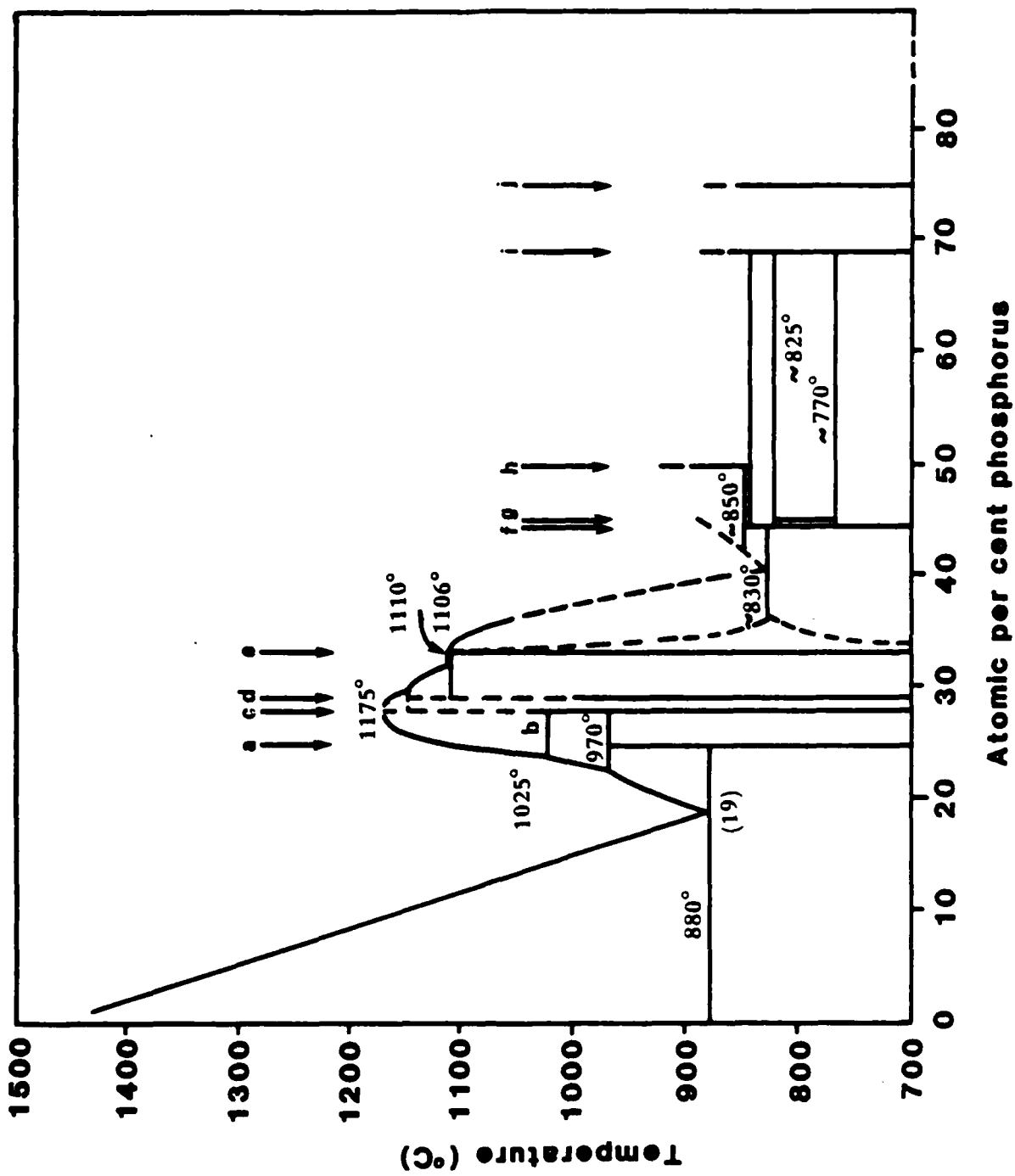


FIGURE 3

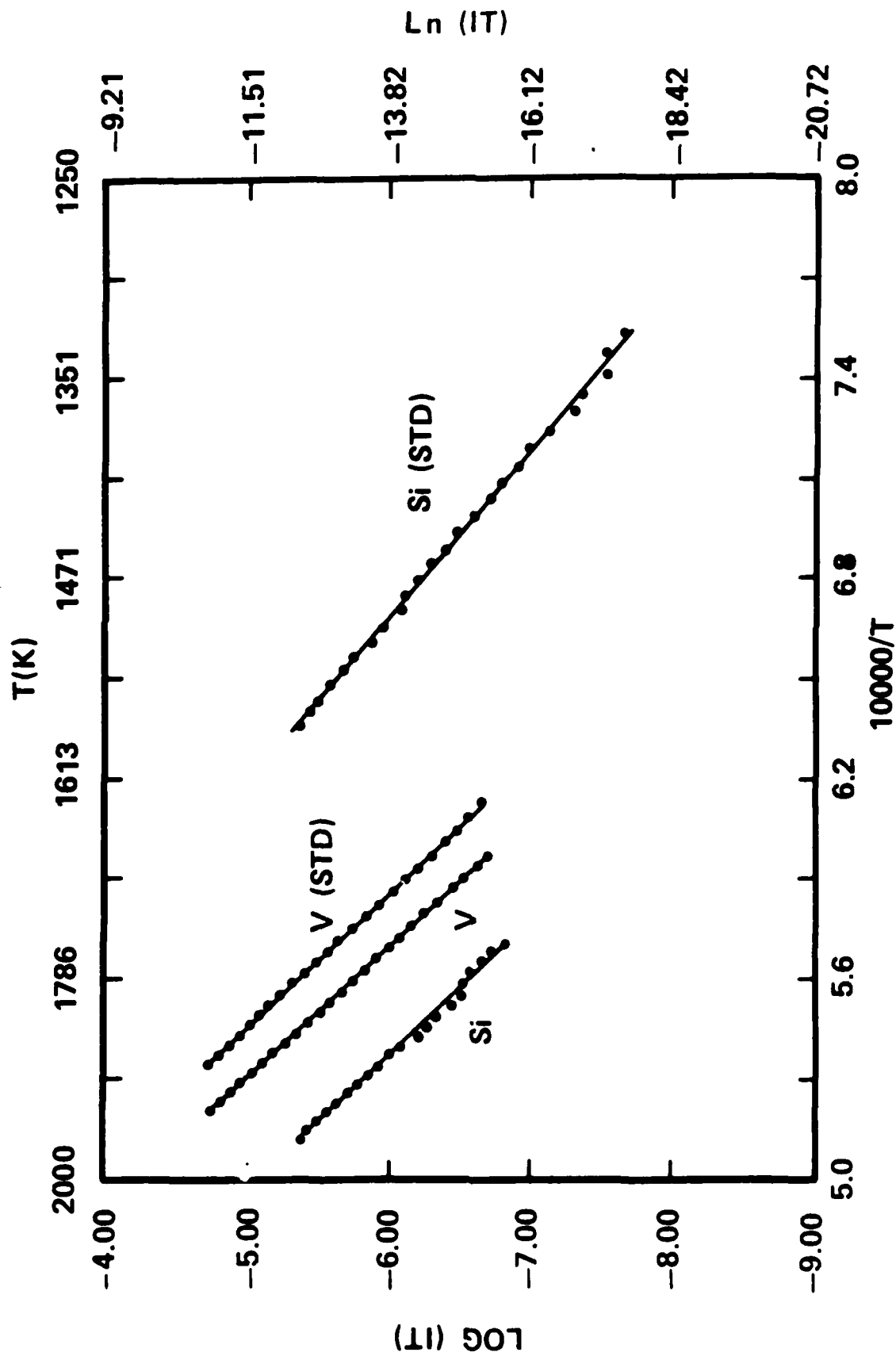


FIGURE 4

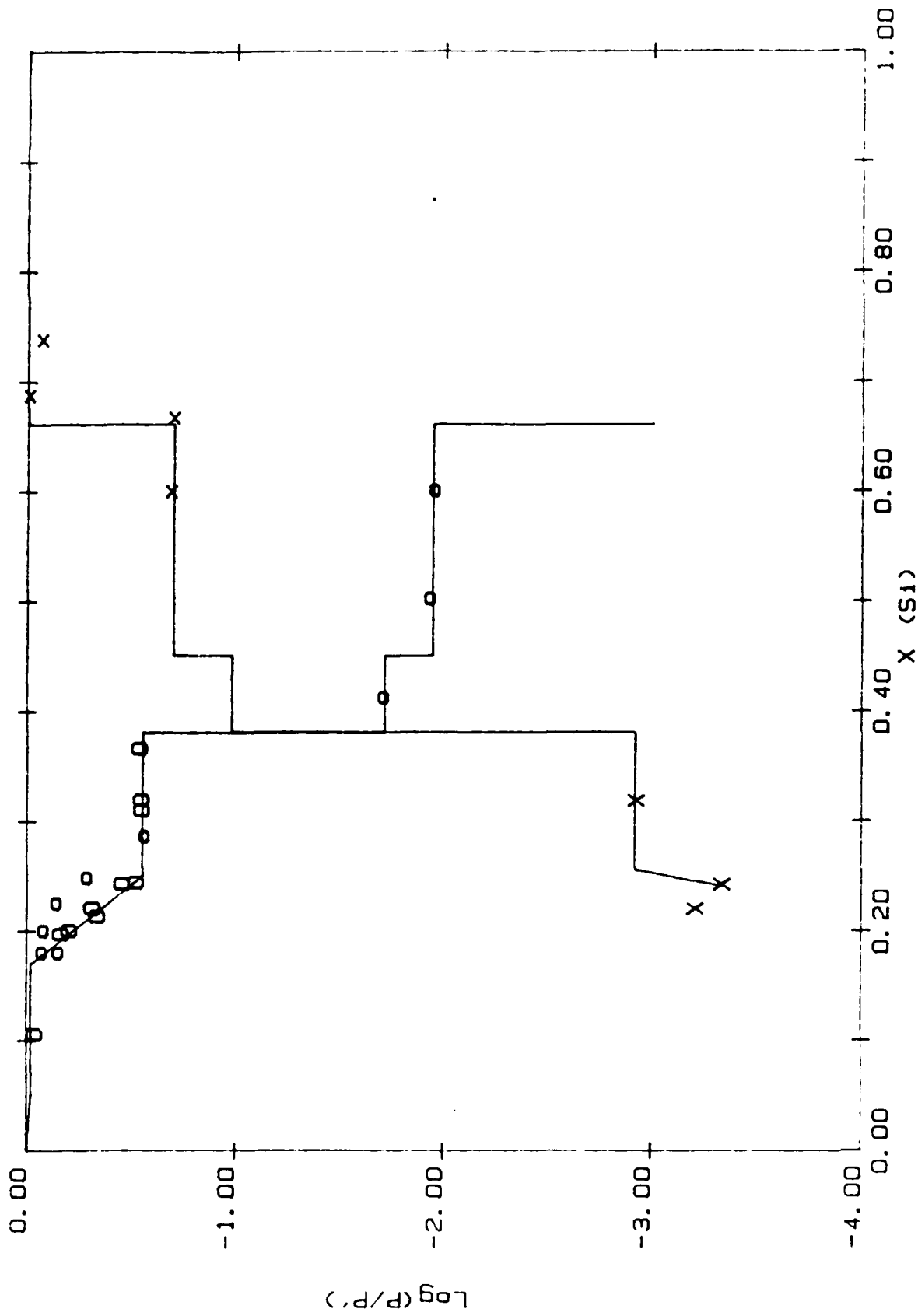


FIGURE 5

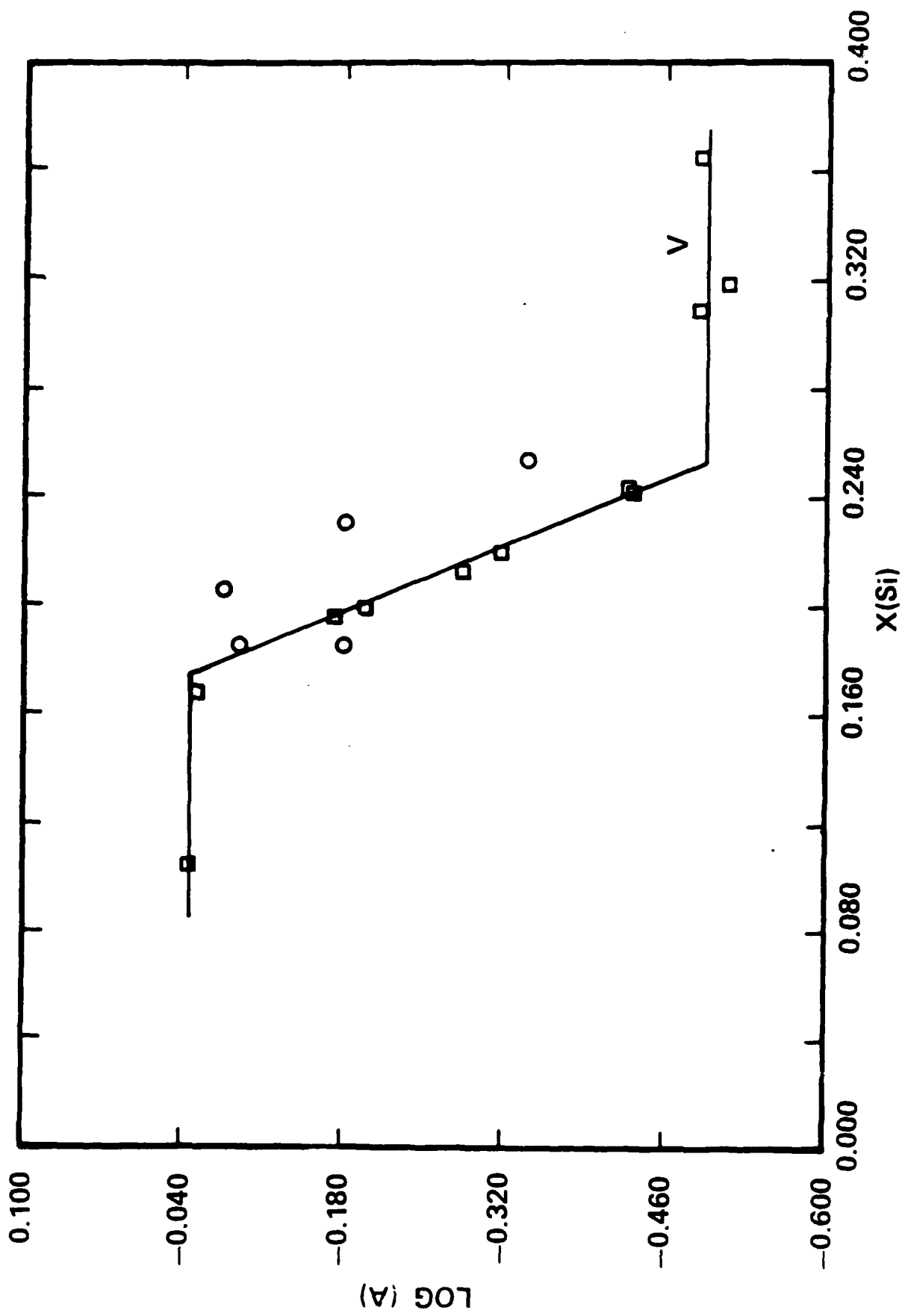


FIGURE 6

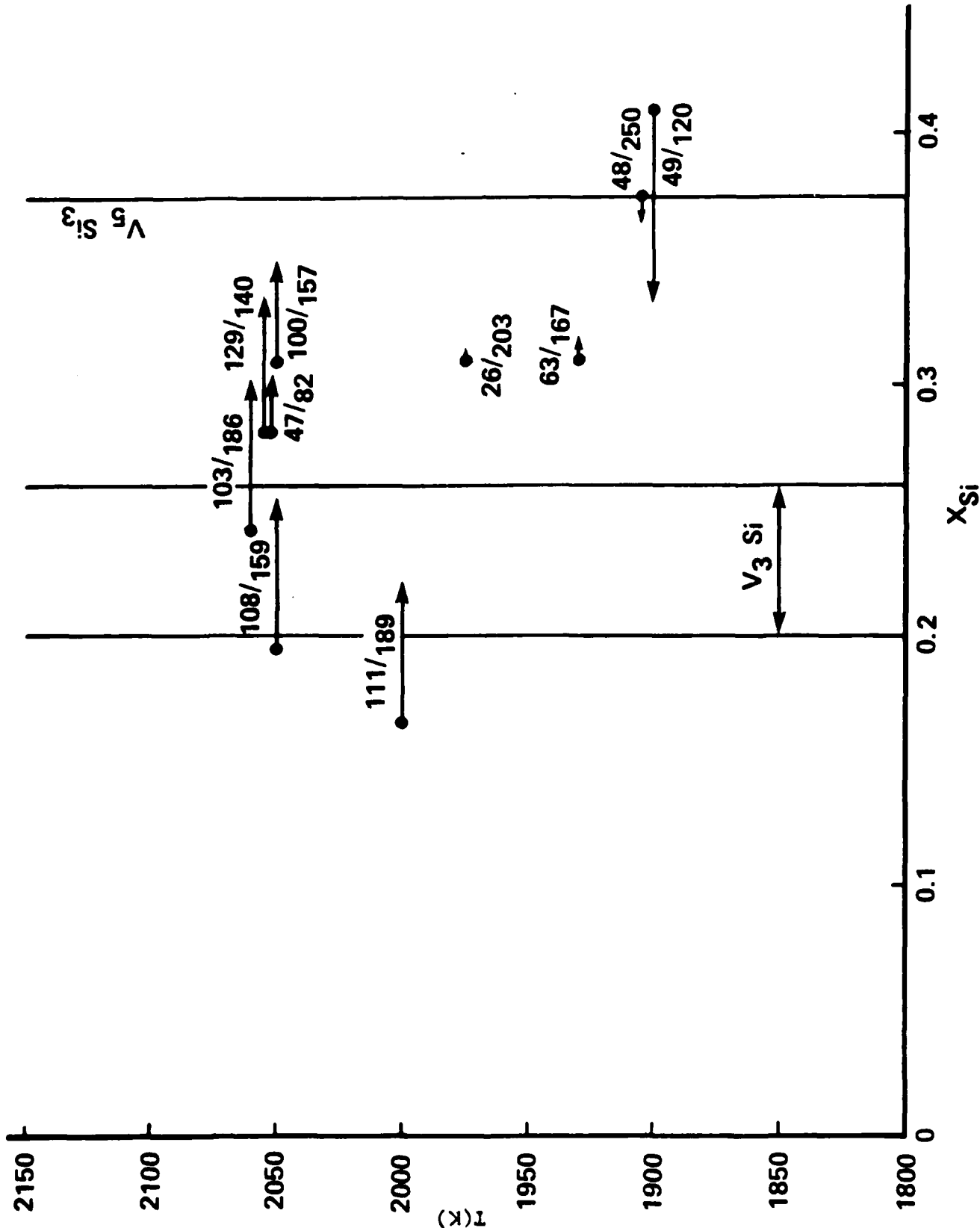
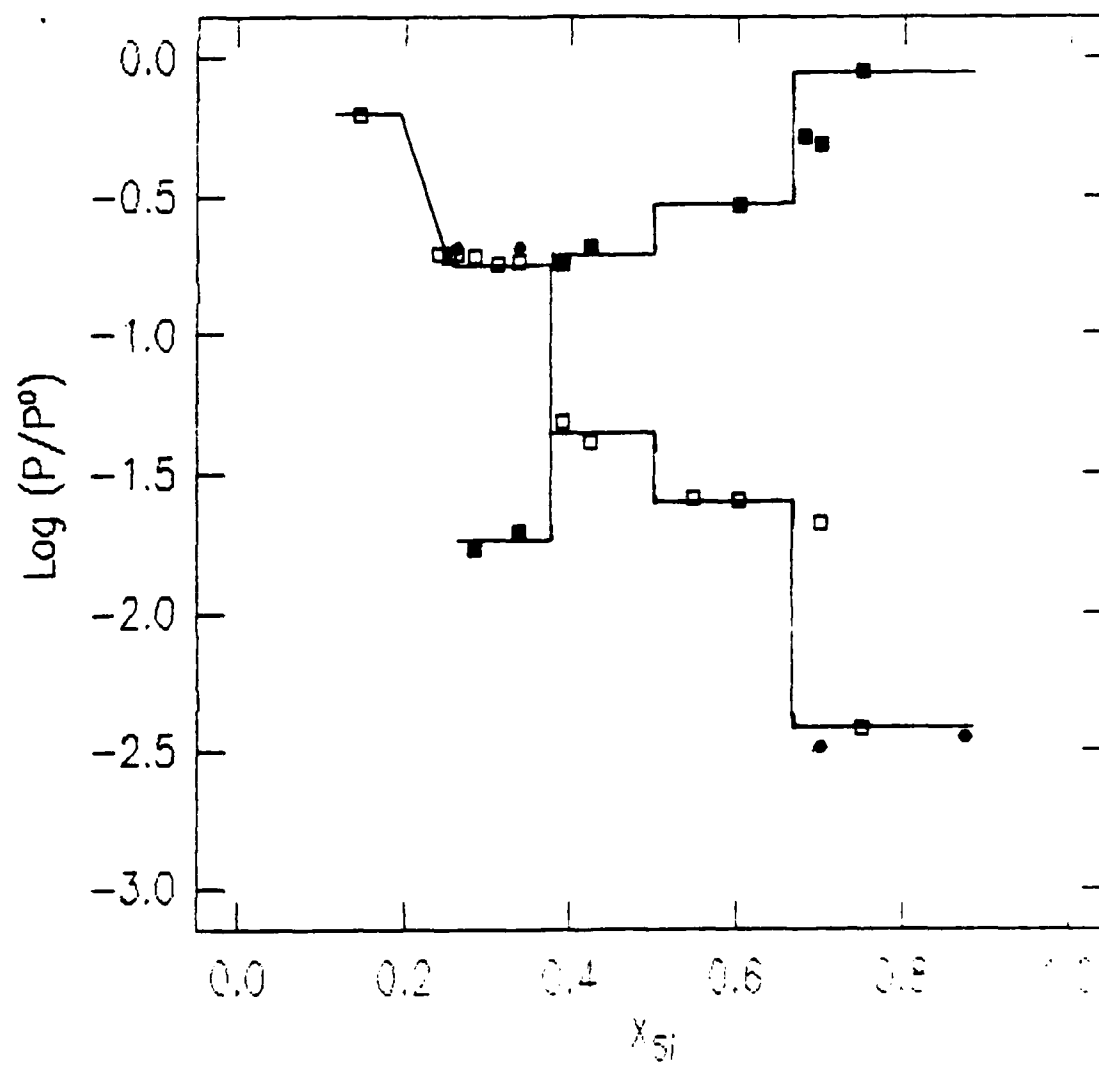


FIGURE 7



Log Activity vs Composition
in the Chromium - Silicon System

FIGURE 8

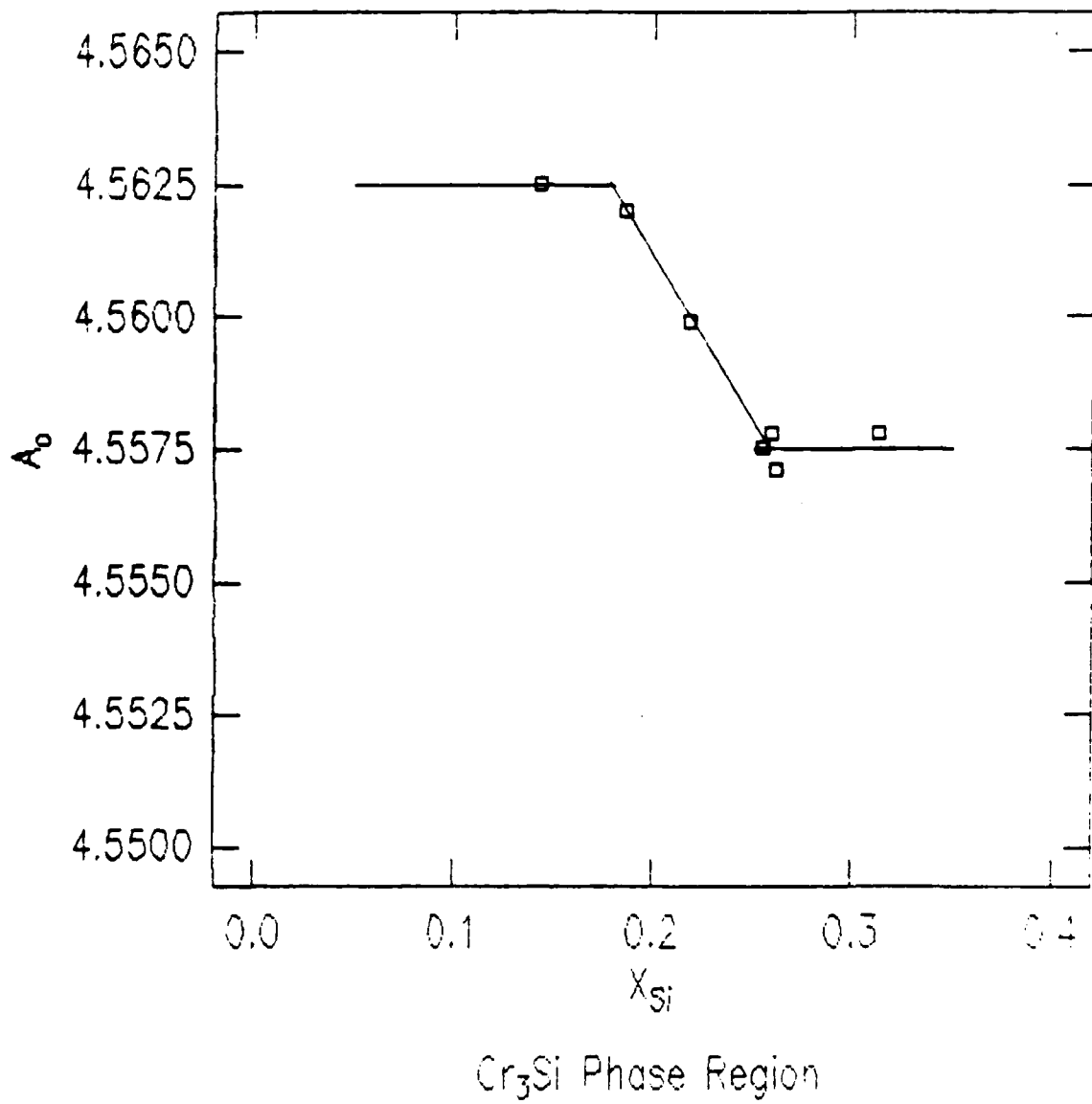
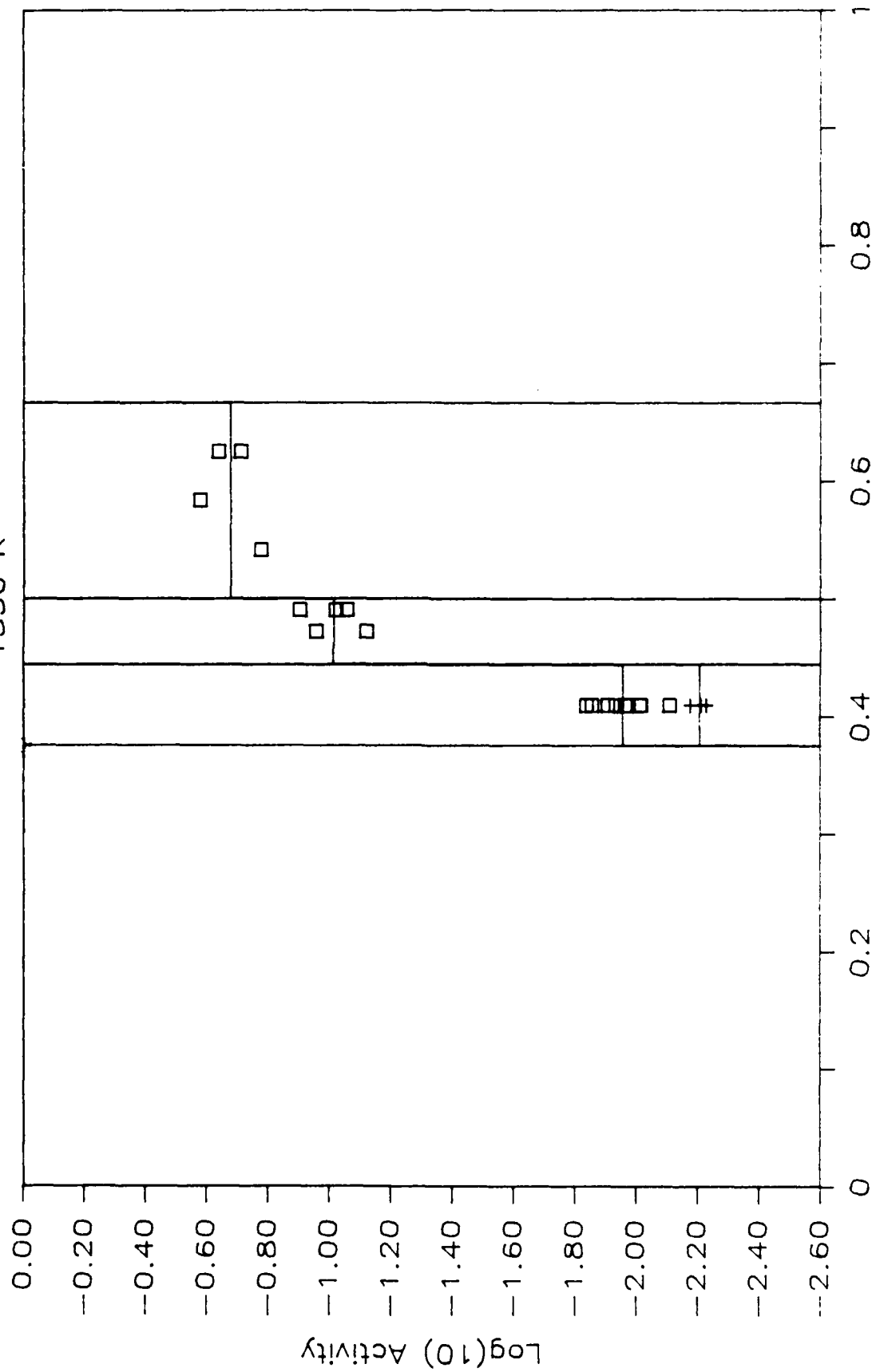


FIGURE 9

Log Activity vs Atom Fraction Si

1550 K



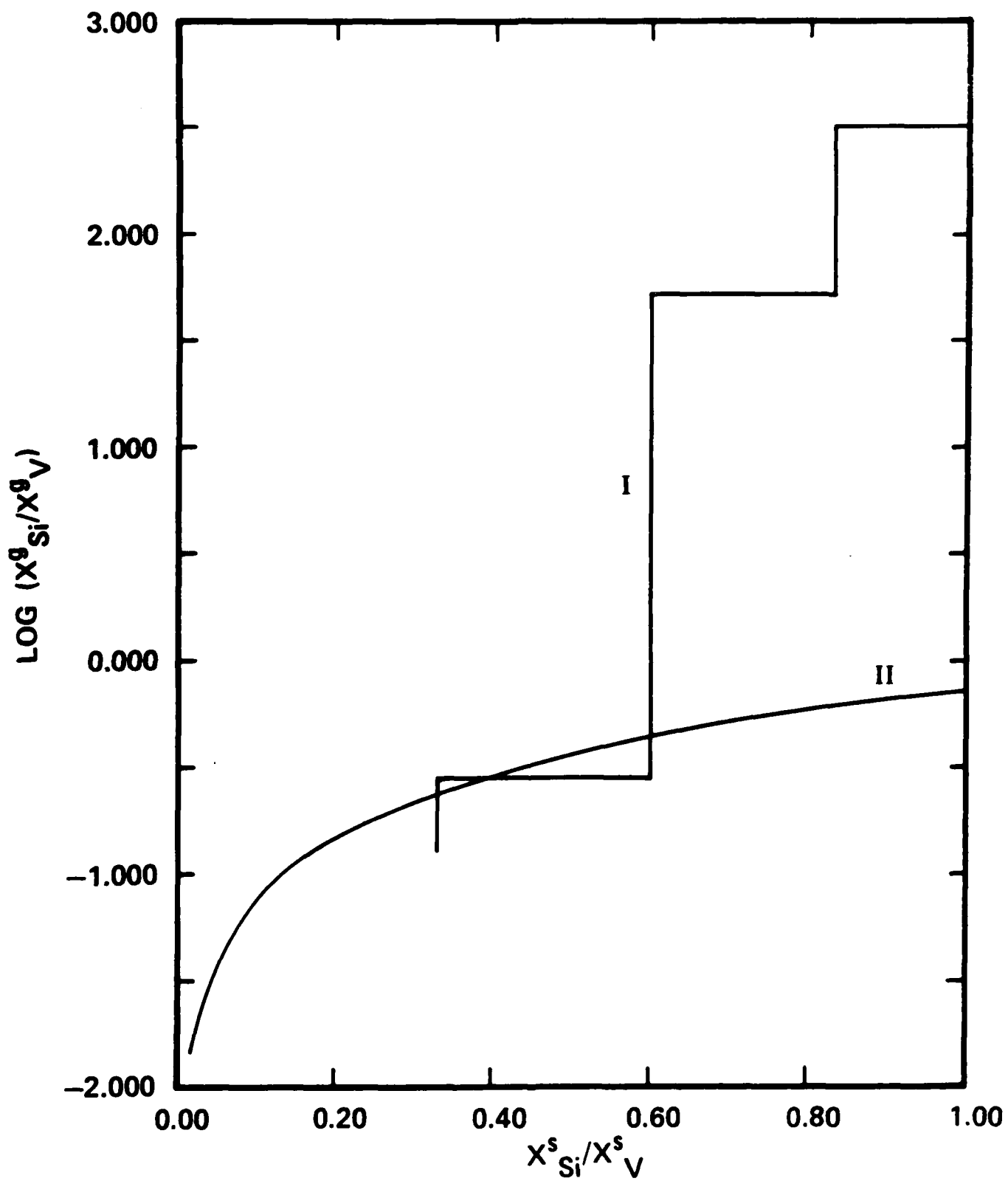


FIGURE 12

ENTHALPIES OF ATOMIZATION

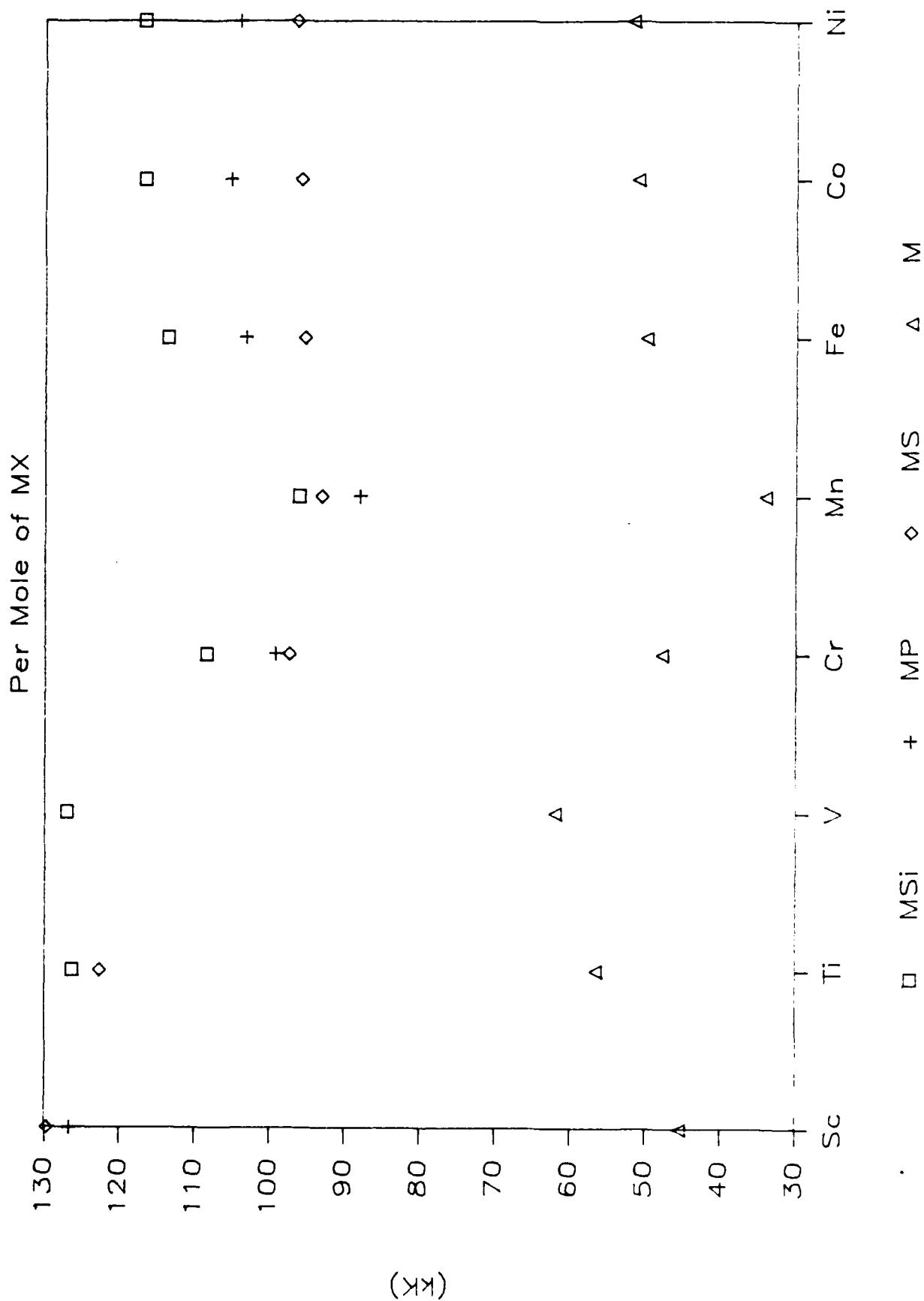


FIGURE 13

ENTHALPIES OF ATOMIZATION

Per Mole of MX; To Valence State M

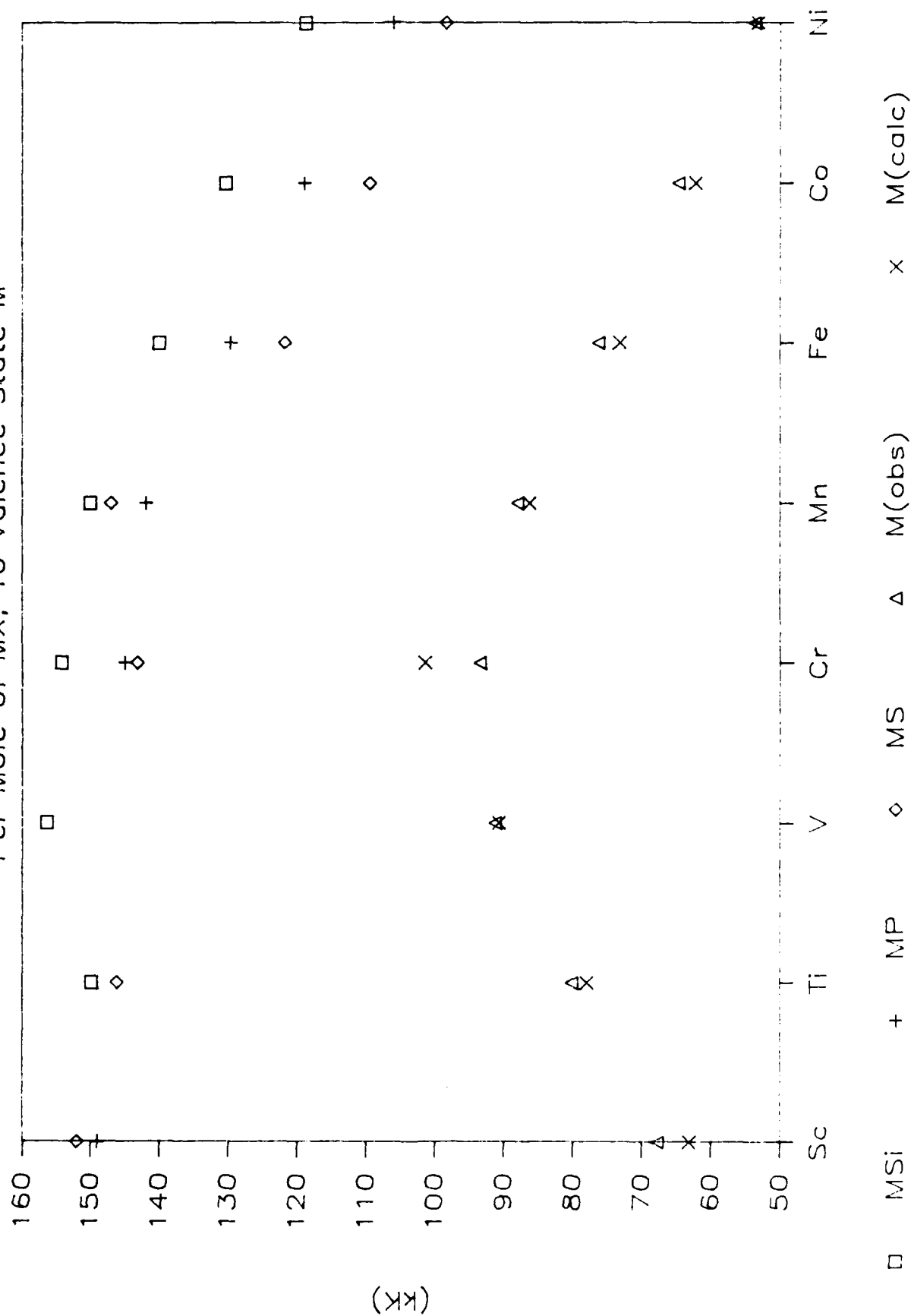


FIGURE 14

ENTHALPIES OF ATOMIZATION

To Valence State Metal Atoms

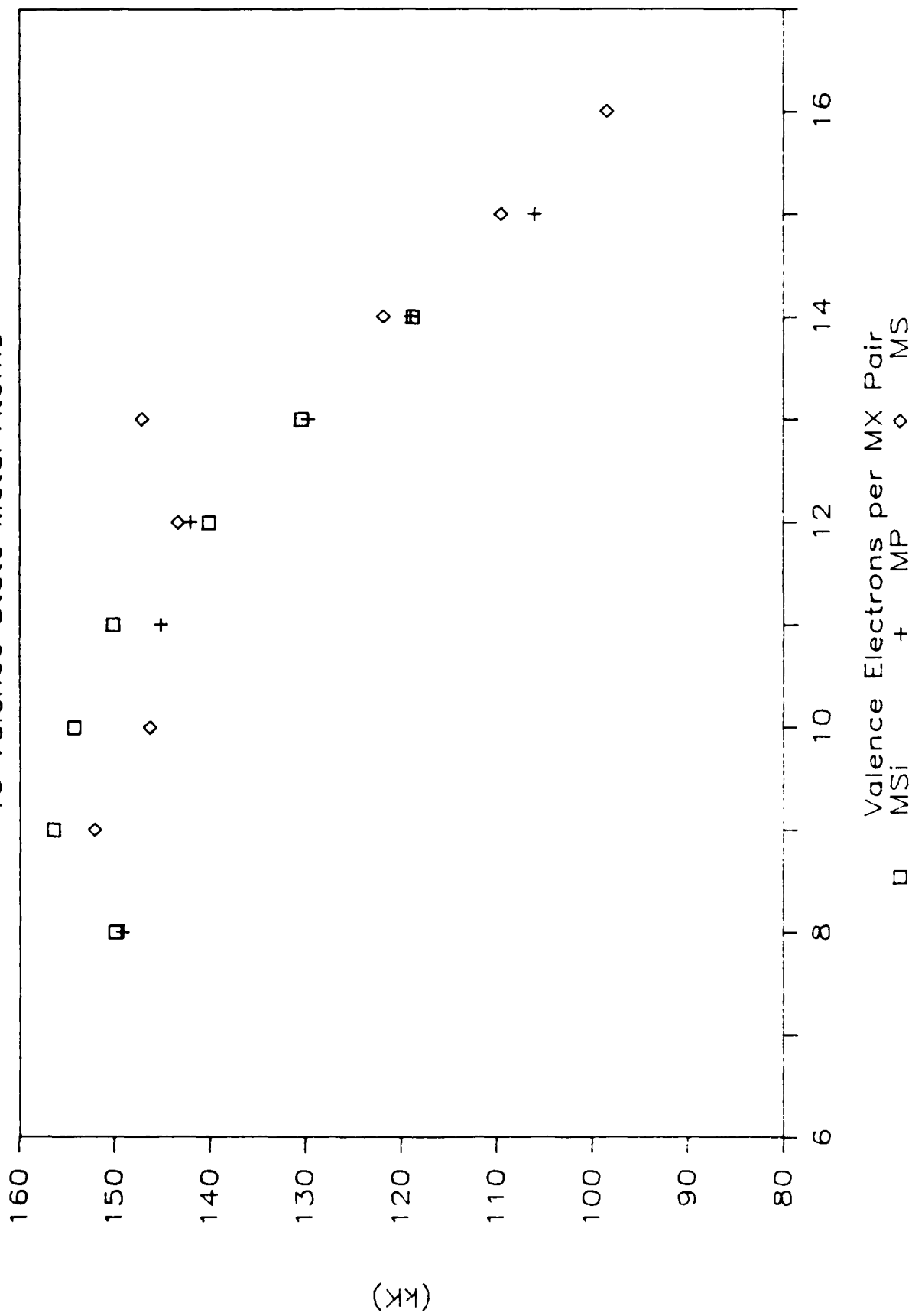


FIGURE 15

END

JAN.

1988

DTIC